PHASE CONTROL IN THE SYNTHESIS OF YTTRIUM OXIDE NANO AND MICRO-PARTICLES BY FLAME SPRAY PYROLYSIS

A Thesis

by

MALLIKA MUKUNDAN

Submitted to the Office of Graduate Studies of
Texas A&M University
in partial fulfillment of the requirements for the degree of

MASTER OF SCIENCE

August 2007

Major Subject: Mechanical Engineering

PHASE CONTROL IN THE SYNTHESIS OF YTTRIUM OXIDE NANO AND MICRO-PARTICLES BY FLAME SPRAY PYROLYSIS

A Thesis

by

MALLIKA MUKUNDAN

Submitted to the Office of Graduate Studies of
Texas A&M University
in partial fulfillment of the requirements for the degree of

MASTER OF SCIENCE

Approved by:

Chair of Committee, Bing Guo
Committee Members, Kalyan Annamalai
Don Collins
Head of Department, Dennis L. O' Neal

August 2007

Major Subject: Mechanical Engineering

ABSTRACT

Phase Control in the Synthesis of Yttrium Oxide Nano and Micro-particles by Flame Spray Pyrolysis. (August 2007)

Mallika Mukundan, B.E., Maharaja Sayaji Rao University of Baroda, India

Chair of Advisory Committee: Dr. Bing Guo

The project synthesizes phase pure Yttria particles using flame spray pyrolysis, and to experimentally determines the effect of various process parameters like residence time, adiabatic flame temperature and precursor droplet size on the phase of Yttria particles generated. Further, through experimentation and based on the understanding of the process, conditions that produce pure monoclinic Y_2O_3 particles were found.

An ultrasonic atomization set-up was used to introduce precursor droplets (aqueous solution of yttrium nitrate hex hydrate) into the flame. A hydrogen-oxygen diffusion flame was used to realize the high temperature aerosol synthesis. The particles were collected on filters and analyzed using X-Ray Diffraction (XRD) and Transmission Electron Microscopy (TEM).

Individual process parameters (flame temperature, residence time, precursor concentration, precursor droplet size) were varied in continuous trials, keeping the rest of the parameters constant. The effect of the varied parameter on the phase of the product Yttria particles was then analyzed. Pre-flame heating was undertaken using a nozzle heater at variable power. Precursor solution concentrations of 0.026 mol/L, 0.26 mol/L,

and 0.65 mol/L were used. Residence time was varied by means of burner diameter (9.5 mm and 1.6 mm ID). Large precursor droplets were removed by means of an inertial impactor.

The higher flame temperatures and precursor heating favor the formation of monoclinic yttrium oxide. The fraction of the cubic phase is closely related to the particle diameter. All particles larger than a critical size were of the cubic phase.

Phase pure monoclinic yttrium oxide particles were successfully synthesized. The end conditions included a precursor concentration of 0.65 mol/L, a pure hydrogen-oxygen flame and a 1.6 mm burner. The precursor droplets entrained fuel gas was passed through a round jet impactor and preheated at full power (130 VA). The particles synthesized were in the size range of 0.350 to 1.7 μm.

DEDICATION

To my parents,

for their unfailing love and support

ACKNOWLEDGEMENTS

I would like to thank Dr. Bing Guo, who gave me an opportunity to work on this project, which has been an immense learning experience. I would also like to thank family and friends, whose support and understanding backed me in successfully completing this project.

TABLE OF CONTENTS

Page

ABSTRACT……..……... iii

DEDICATION……. v

ACKNOWLEDGEMENTS……. vi

TABLE OF CONTENTS…… vii

LIST OF FIGURES……. ix

LIST OF TABLES……... xi

1. INTRODUCTION……... 1

2. EXPERIMENTAL SET-UP…… 7

Gas Supply and Regulation……..……. 7
Atomization Setup…….……..... 8
Impactor Design…..…….. 8
Synthesis Setup…….…… 8
Sampling/Collection Mechanism…..…… 9

3. RESULTS AND DISCUSSION…..…..……... 11

Effect of Flame Temperature ……... 12
Effect of Precursor Pre-heating……. 13
Effect of Residence Time……...……... 14
Effect of Precursor Concentration……...…….. 14
Effect of Particle Size……..……. 16
Summary of Results…….. 20

4. CONCLUSION…….……..... 21

REFERENCES…… 22

APPENDIX A …… 24

APPENDIX B …… 30

APPENDIX C …… 34

Page

VITA…… 65

LIST OF FIGURES

FIGURE		Page
1	Schematic showing the flame spray pyrolysis setup…..……	45
2	Photograph showing the synthesis chamber set-up…..……...…	46
3	Photograph showing the co-flow burner and the synthesis flame……...	47
4	Representative XRD result showing cubic and monoclinic Yttria mixture …….....	48
5	XRD result showing pure monoclinic Yttria sample (0.65 mol/L precursor concentration, full power nozzle heating)..……	49
6	XRD result (No pre-heating, 0.26 mol/L concentration, 1.6 mm burner).....	50
7	XRD result (60VA pre-heating, 0.26 mol/L concentration, 1.6 mm burner)…….	51
8	XRD result (full power pre-heating, 0.65 mol/L concentration, 1.6 mm burner)..……....	52
9	XRD result (9.5 mm burner, 0.65 mol/L concentration, full pre-heating)……..…….	53
10	XRD result (Full pre-heating, 0.26 mol/L concentration,1.6 mm burner)……..…....	54
11	XRD result (Full power pre-heating, 0.026 mol/L concentration, 1.6 mm burner)……...……...	55
12	TEM images showing measured particle size effect for Y_2O_3…….....	56
13	Graph showing size effect (Results from measurement for over 50 individual particles obtained using TEM and SAED……	57
14	TEM image showing particle size distribution……..	58
15	Histogram showing particle size distribution with and without using an impactor……...	59

FIGURE		Page
16	3D domain of the impactor (mesh image from gambit)…….	60
17	Image from Gambit showing mesh quality…….....	61
18	Fluent image showing 3D velocity profile at the impactor mid-plane.....	62
19	Fluent image showing smaller sized particle tracks (1 µm) through the impactor……	63
20	Fluent image showing larger sized (10 µm) particle tracks……...	64

LIST OF TABLES

TABLE		Page
1	Bill of Materials…….	39
2	Estimated Adiabatic temperature of $H_2/O_2/H_2O$ (H_2O as a liquid in starting fuel gas) flames…….	40
3	Particle size distribution before using an impactor (Yttria particles synthesized by flame spray pyrolysis at H_2 at 1slm and O_2 at 5 slm, 0.65 mol/L concentration, full power nozzle heating)……...	41
4	Particle size distribution after using an impactor (Yttria particles synthesized by flame spray pyrolysis at H_2 at 1slm and O_2 at 5 slm, 0.65 mol/L concentration, full power nozzle heating)……...	42
5	Simulation Results…….	43
6	Summary of experimental results …….	44

1. INTRODUCTION

The generation and study of micro and nano particles is a field which is drawing considerable attention in recent times. The interest in these microscopic particles arises from the special properties that they exhibit due to their small size. A large number of optical, catalytic, electrochemical, melting and magnetic properties are size dependent (Rosner, 2005).

Properties of these particles are usually significantly different from those of bulk material. Particle research thus seeks to exploit the strong size dependence of the physical and chemical properties of microscopic particles. This opens up the opportunity to create materials with entirely new characteristics. These particles find applications in the field of ceramics, catalysis, fuel cells, electronics, chemical–mechanical polishing, data storage, or coatings (Ichinose et al., 1992; Kruis et al., 1998, Rittner, 2002).

The challenges in the field are to find methods of synthesis of these particles on a commercial scale. Other challenges include synthesis of particles with controlled characteristics of size, phase, morphology, composition and good levels of purity. A number of techniques have been used to generate these particles namely sol-gel technique, hydroxide precipitation, hydrothermal synthesis, laser heated evaporation, gas phase synthesis and flame spray pyrolysis (Ichinose et al., 1992)

This thesis follows the format of *Aerosol Science and Technology.*

The gas phase synthesis technique is an aerosol technique for powder synthesis. The technique is used to generate a large variety of micro, nano particles of interest. In this process, the appropriate precursor vapor /gas is mixed with a fuel (e.g. Acetylene or methane) and oxygen. The mixture is burnt through a specially designed burner. The precursor decomposes in the flame and nano particles are nucleated. The synthesized particles are then collected by using a suitable method of capture. By proper choice of precursors the different nano materials that may be synthesized is almost limitless (Tok et al., 2007).

The gas phase synthesis is a preferred method compared to a number of other methods of nano particle generation (Rosner, 2005). The gas phase synthesis is a very economical process as compared to a number of techniques. The heat of combustion is available to oxidize the precursor vapors, there are number of process control parameters like the flame temperature, residence time and diluents to oxygen ratio which are used to control the particle morphology and size (Guo et al., 2006).The gas phase synthesis method achieves in a single step what the wet-chemical methods can achieve in several steps. It is also capable of a high production rate. The gas phase synthesis is thus a very successful process. It is commercially used to produce a number of metal oxides and substances like carbon black. However, it is popularly used to synthesize oxides because of the basic oxidizing nature of a flame.

The gas phase process however suffers from a number of limitations. It is a preferred method when the precursor has a low vapor pressure or can be easily vaporized. This however puts a limitation on the number of substances which can be used as a precursor.

The process is inherently two stepped as it involves the vaporization of precursor and the introduction of its vapors into the flame. This increases the time required for the entire process.

The process of flame spray pyrolysis is a variant of aerosol techniques used for powder synthesis, which tries to overcome some of the problems associated with gas phase synthesis. This process involves the introduction of finely subdivided liquid precursor droplets into the flame instead of injecting the precursor vapors. These droplets are subsequently transported through the flame, in which the solvent evaporates and the dissolved species react to form product particles. It thus allows the use of precursors having high vapor pressures and expands the scope of flame synthesis to using a variety of precursors and in turn producing a variety of new materials.

Flame spray pyrolysis is a continuous process and it has the following advantages (Lenggorro et. al., 2000).

- The process is preferred for synthesis of spherical particles however can be used to synthesize particles of varied morphology (Rosner, 2005).
- The distribution of diameters is controllable from μm to submicron range.
- The purity of the product is high.
- It has minimal post processing in comparison to other wet methods of powder synthesis.
- It is ideal for commercial application in view of its low cost and continuous operation and minimal post processing.

Flame spray pyrolysis however has its own problems (Tok et al., 2006). There are problems of agglomeration. Special burners and gas flow configurations are required for fuel oxidizer mixing, as these factors affect the final product form. The control of particle characteristics during flame synthesis is important because the properties of materials made from these particles depend on size and size distribution, morphology, extent of aggregation and chemical and phase composition of the particles (Pratsinis, 1998)

In addition FSP has challenges with the type and characteristics of the nebulizer used to atomize the precursor solution. The main challenge lies in control of the droplet generation rate and droplet size as they both affect the morphology of the final generated particles (Tok et al., 2006). Most atomization techniques produce droplets in a large size range, which makes the control of particle size within a small range difficult. Other problems include the choice of the method of atomization with reference to the precursor viscosity.

Ultrasonic atomization is a promising technique to be used in conjunction with flame spray pyrolysis. It involves a liquid surface that is set into vibrating motion (triggered by a piezo crystal) such that the direction of vibration is perpendicular to the surface; the liquid absorbs some of the vibration energy, which is transformed into standing waves. With increase in the amplitude of vibrations of the piezo the amplitude of oscillations at the liquid surface also increases and at the critical amplitude the liquid atomizes into droplets. The amount of liquid atomized by atomizer can be controlled by the liquid feed

rate to the atomizer. Thus the characteristics of ultrasonic atomization well complement the needs of the FSP technique and they form a potentially beneficial combination.

It is always of interest to generate new materials with novel applications. Yttria is one such material. Yttrium oxide occurs in two main phases the C-type cubic phase and the B-type monoclinic phase. The stable phase of occurrence at room temperature and pressure is the cubic phase. The monoclinic phase is also called the high temperature phase; it is a metastable state which means it is thermodynamically unstable at room temperature.

Yttrium oxide is used as a hosting material for phosphors and these are synthesized by the flame spray process. The monoclinic phase is invariably formed in this process and it is undesirable. Thus by controlling conditions to synthesize phase pure Yttria by the flame spray process we can arrive at the conditions we need to avoid to prevent formation of the monoclinic phase.

These cubic and monoclinic Yttria particles are also used in research applications such as the interplay between polymorphism and surface energy of metal–oxide nanoparticles (McHale et al., 1997, Navrotsky et al., 2003) and making optical materials with transparency in the long-wavelength edge of the infrared spectrum (Willingham et al., 2003).

It is known that very high temperatures are required for synthesis of monoclinic Yttria. There has been lot of study about the effect of various parameters on the morphology and size range of gas phase generated Yttria particles (Chang et al., 2004) but there has been little investigation about how to control the various parameters to synthesize particles of a particular phase.

It is thus of interest to see if Yttria particles in sizeable quantities could be generated by the process of flame spray pyrolysis and also if their phase could be controlled.

In this study, phase control in FSP is demonstrated by synthesizing phase pure monoclinic Yttria by varying various parameters like precursor concentration, residence time, flame temperature, precursor pre-heating and droplet size using ultrasonic atomization.

2. EXPERIMENTAL SET-UP

The experimental set-up consists of an aerosol synthesis apparatus and a vacuum pump driven sampling/collection apparatus. Figure 1 shows a schematic for the set-up and Figure 2 shows a picture of the apparatus during experimentation. The synthesis apparatus consists of a co-flow burner which uses hydrogen gas as the fuel and pure oxygen gas as the co-flow. Atomized precursor droplets are introduced into the fuel gas stream at a constant rate. The atomized droplets undergo nucleation, evaporation and crystallization in the flame to give our powders of interest. The entire apparatus can be classified into the following categories: gas supply and regulation, atomization, synthesis and aerosol sampling/collection.

Gas Supply and Regulation

The experiment uses hydrogen as the fuel gas and pure oxygen as a co-flow. Hydrogen (part no. HY 4.5, product grade-4.5 with 99.995% purity, supplier: Praxair) and Oxygen (part no. OX 2.6, product grade-2.6 with 99.6% purity, H_2O< 10 ppm, supplier: Praxair) used are of industrial grade purity. Nitrogen (part no. NI 4.8, product grade-4.8 with 99.998% purity, supplier: Praxair) was used in the process to purge the supply lines with an inert gas to eliminate the potential hazard of the combustible mixture. The gas supply was regulated using mass flow controller (MKS, Wilmington MA, 1179A) and monitored using a mass flow meter (MKS, Wilmington MA, 179A). It is a high accuracy device (+/- 0.026 mol/L F.S.) which helps in setting gas type, range, correction factors and gas flow rate.

Atomization Set-up

The atomization set-up consists of a 1.7 MHz piezo crystal which is kept submerged in water for correct operation (Figure 1). The atomization vessel has a thin film (Glad Clingwrap, Oakland, CA) mounted at the bottom. The film is in contact with the water surface. The piezo crystal transfers the ultrasonic vibrations to the water. The atomization vessel is made of stainless steel (0.11m) and has a (Cole-Parmar, Vernon hills, IL, 75900-00,-05) syringe pump connected at one end to maintain supply of precursor solution at a constant rate of 5ml/hr. The fuel gas flows at a constant rate of 1 L/min and carries with it the atomized droplets into the flame.

Impactor Design

Inertial impactor is a device widely used for the sampling and size-selective collection of aerosol particles. Their principal of operation is simple: an aerosol stream passes through a nozzle and impinges upon a collection plate. Particles in the aerosol stream having large enough inertia will impact upon the collection plate while the other particles will follow the flow stream out of the impaction region. A stainless steel single stage round jet impactor, machined in-house, with nozzle diameter of 2.87 mm and the nozzle plate distance of 3.30 mm was used to remove large size droplets entrained in the flow path of the fuel gas.

Synthesis Setup

The synthesis setup consists of a co-flow burner using a 1.6 mm and 9.5 mm ID nozzles (Figure3) .The co-flow burner consists of a main fuel flow channel surrounded by a co-

flow annulus. A nozzle heater (type HBA, Chromalox Inc., PA) was used to preheat the precursor droplets carried by the fuel gas. A single phase 0-130VA transformer was used to vary the heating effect to be provided to the nozzle. A K type thermocouple (Omega Instruments, Stamford, CT) was used to measure the outer temperature of the burner. The thermocouple is connected to a digital temperature indicator. The thermocouple is mounted with its probe in contact with the area between the burner and the heater.

The furnace is made of stainless steel, 35mm in length and 38.1/14.6mm in outer/inner diameter. It is fitted inside a Chromalox HBA-31427 coil electric heater. The stainless-steel cylindrical burner is mounted on the top centre of the furnace. Replaceable burner mouths with inner diameters of 1.6mm and 9.5mm were used to render different residence times

Precursor Selection

In flame spray pyrolysis, the precursor composition is a key parameter to control the particle content and properties. A water solution of Yttrium nitrate hex hydrate (CAS # 13494-98-9) was used as precursor for our experiment. It is a corrosive substance and is also an oxidizer and an irritant. It hence needs to be stored according to the MSDS specifications.

Sampling /Collection Mechanism

A vacuum pump (BOC Edwards, Wilmington, MA) provided the suction to draw the post-flame aerosol into the sampling tube. It is a rotary vane pump with a 3.7m^3/hr of displacement at 50 Hz operation. The aerosols are drawn into a 1/4" OD stainless steel

sampling tube. The sampling tube is attached with a special filtration unit. It consists of a 47mm stainless steel filter holder (Pall Corporation, East Hill, NY). It has a closed system connection with an internal dispersion chamber. The particles are trapped on an alumina membrane filter (Anodisc, Whatman, Florham Park, NJ.) The 47mm diameter and 0.1 and 0.2 micrometer pore sizes were used. Table 1 shows the bill of materials of all parts classifying them into bought and manufactured components.

3. RESULTS AND DISCUSSION

In flame spray pyrolysis a number of phenomena occur when a precursor droplet converts to a product particle. There is evaporation of water followed by the processes of nucleation and crystallization of the precursor $Y(NO_3)_3.6H_2O$, loss of water of crystallization from the precursor particle followed by the melting and decomposition of $Y(NO_3)_3$. The final changes include melting, nucleation and crystallization of Y_2O_3. The study of flame spray pyrolysis brings out the major control parameters which play a role in the final particle phase. It is the simultaneous monitoring of all these parameters that gives us some control over the end-product.

The following parameters were varied individually in course of the experimentation and the effect on the phase of the end product was analyzed:

- Flame temperature
- Precursor Pre-heating
- Residence Time
- Precursor droplet size / Particle size

The phase controlled end-sample that was successfully synthesized was pure monoclinic with base-centered crystal structure. The particles were in a size range of 0.350 to 1.7 μm. The synthesized samples were analyzed using the XRD technique for study of crystal structure and TEM for study of crystal structure, size and morphology.

Figure 4 shows a representative XRD image of a mixture of cubic and monoclinic particles of Yttrium oxide. The cubic to monoclinic particles in our samples were estimated by taking a ratio of peak heights of the cubic peak at 2-theta 29.15 degrees to the monoclinic peak at 2-theta 28.587 degrees. Fig 5 shows a representative XRD image of pure monoclinic yttrium oxide. It is seen that it has no cubic peaks.

Effect of Flame Temperature

It is known that a sufficiently high temperature is essential for the synthesis of monoclinic yttrium oxide. The adiabatic flame temperatures for different H_2O-H_2 ratios have been calculated for a laminar diffusion flame used for gas phase synthesis of Yttria. Table 2 shows the estimated adiabatic temperature of $H_2/O_2/H_2O$ (H_2O as a liquid in starting fuel gas) flames (Guo et al., 2006). It is seen from the table that as the H_2O-H_2 molar ratio increases the flame temperature drops. So knowing that a sufficiently high temperature is required for our synthesis (such as 3027 K) an H_2O-H_2 molar ratio of 0.1 would have to be maintained.

In our experiment a sufficiently high temperature was maintained in two ways. Firstly the fuel gas was burnt in a pure oxygen flame; no other gases were used as diluents. In addition the precursor feed rate to the atomizer was maintained at a constant rate of 5 ml per hour. The atomizer was hence operated under its full capacity. This was also done in an effort to maintain the H_2O-H_2 molar ratio to 0.1. As the fuel gas was supplied at a constant rate of 1 liter per minute, increasing the precursor feed rate above 5 ml per hour would push more water into the flame and hence lead to a drop in the flame temperature.

Effect of Precursor Pre-heating

Pre-heating the precursor refers to increasing the temperature of the precursor droplets to start out the processes of evaporation and decomposition of the precursor even before they enter the flame.

The fuel gas with entrained precursor droplets was made to pass through a pre-heating section consisting of a nozzle heater. The effect of precursor pre-heating was analyzed by starting out with no pre-heating followed with pre-heating at different power settings. The full power heating (130 VA) heats the nozzle to a temperature of 500C.

The XRD result (Figure 6) of the 'no-preheating' sample showed a high cubic to monoclinic ratio of 2.0. A trial was carried out with pre-heating at 60 VA and Figure 7 shows the XRD result for the resultant sample. It gave a cubic to monoclinic ratio of 0.9. Another trial was carried out using pre-heating of 130 VA (full power). Figure 8 shows the XRD result for the synthesized sample, it had a cubic to monoclinic ratio of 0.7 which was significantly lower.

It was hence seen that pre-heating the precursor had a significant effect in reducing the cubic to monoclinic ratio. With pre-heating there is an early start of evaporation. The evaporation is followed by decomposition of the precursor. An already heated droplet entering the flame acts towards increasing the adiabatic flame temperature. Thus the pre-heating of the precursor favors the formation of monoclinic yttrium oxide.

Effect of Residence Time

The furnace residence time is defined as the volume of the furnace divided by the flow rate of fuel gas. In our experiment as the flow rate of fuel gas was maintained constant, the furnace residence time was varied by using different cross-section burners. Burners with 9.5 mm and 1.6 mm ID were used for this purpose.

Keeping other conditions constant a trial was run using the 9.5 mm ID burner. Figure 9 shows the XRD result of the synthesized sample. It gave a cubic to monoclinic ratio of 0.6. A was run using the 1.6 mm ID burner. Figure 10 shows the XRD result of the synthesized sample. It gave a cubic to monoclinic ratio of 0.5.

It was seen that there was no significant difference of using different sized burners. This was attributed to the fact that there is no significant difference in the residence times for the particles between the two burners dimensions used, in comparison to the time required for phase change of Yttria.

Effect of Precursor Concentration

The precursor concentration was varied and its effect on the phase of the resultant particles was analyzed. The water solutions of yttrium nitrate hex hydrate with molar concentrations of 0.026, 0.26 and 0.65 mol/L respectively were used for this purpose.

A trial was carried out keeping rest of the conditions constant and using a precursor of 0.65 mol/L molar concentration. Figure 8 shows the XRD result of the synthesized sample. It gave a cubic to monoclinic ratio of 0.7.

Similarly a trial carried out with the 0.26 mol/L concentration precursor. Figure 10 shows the XRD pattern for the generated sample. It has a cubic to monoclinic ratio of 0.5. Figure 11 shows the XRD pattern for a sample synthesized with the 0.026 mol/L precursor solution and it has a cubic to monoclinic ratio of nearly zero, the sample is nearly phase pure monoclinic.

Hence it was seen that the precursor concentration has a significant effect on the cubic to monoclinic ratio. With the decrease in the precursor concentration the cubic to monoclinic ratio also decreases. It was also seen that the change in the cubic to monoclinic ratio is not significantly different between the 0.65 mol/L concentration sample and the 0.26 mol/L concentration sample but is appreciably higher than the 0.026 mol/L concentration sample.

The precursor concentration has a direct relationship to the resulting particle size. The size of the synthesized Yttria particle has a directing bearing on its phase (discussed in the next section). Particle size is directly proportional to the cube root of the concentration of the precursor solution used for synthesis ($D_p \propto \sqrt[3]{C}$, where, D_p is the particle size, and C is the precursor solution concentration.) Thus when the precursor concentration is changed from 0.65 mol/L to 0.26 mol/L the particle size decreases by a

factor of 1.36 and there is hence not a significant difference on the cubic to monoclinic ratio. However when the precursor concentration is changed from 0.26 mol/L to 0.026 mol/L the particle size decreases by a factor of 2.16 which appreciably drops the cubic to monoclinic ratio.

Though the 0.026 mol/L solution gives phase pure monoclinic yttrium oxide particles it gives a very low production rate. Hence to produce phase pure monoclinic Yttria in sizeable quantities the control of droplet size becomes critical.

Effect of Particle Size

A study of individual Yttria particles synthesized using TEM with Selected Area Electron Diffraction (SAED) showed that the particle size has a close bearing on the phase of the synthesized particle (Guo and Luo, 2007). Figure 12 shows the individual TEM images for the cubic and monoclinic samples. It was found that particles that were larger than a certain critical size were all of the cubic phase. Figure 13 is a graph which pictorially shows the same result and was plotted after study of 50 individual particles using TEM and SAED.

Realizing that the particle size is critical it was understood that it had to be controlled. This was done in two ways. Firstly by controlling the precursor concentration as discussed already.

The second method was to control the size of droplets entering into the flame and this was done using a round jet inertial impactor. Keeping the rest of the parameters constant and a precursor concentration of 0.65 mol/L, a round jet impactor was introduced in the flow path of the atomized droplets. The resultant sample was analyzed using XRD and the particles were found to be phase-pure monoclinic (Figure 5). The TEM images for the particles collected were studied and a size distribution ranging from 0.1-1.1 μm was obtained (Figure 14). The particle size distribution was studied by measuring particle sizes using METAMORPH (MDS Inc., Toronto, Canada).Table 3 shows the size distribution of particles before using the impactor while Table 4 shows the particle size distribution after using an impactor. The larger particle sizes over 1.1 μm were not detected in the sample after the use of an impactor.

Figure 15 is a histogram which shows the particle size ranges with and without using an impactor. There is a significant shift in the particle sizes towards the smaller size ranges after using an impactor.

Knowing that the impactor was removing the larger sized droplets from entering the flow path of gas, it was of interest to quantify its collection efficiency. It was also of interest to see the nature of flow through an impactor and for this a numerical analysis was carried out.

Characterization of droplet flow through the inertial impactor

An analysis of the droplet laden flow was carried out to characterize the two-phase flow and hence help in selection of a suitable numerical scheme for use in simulation. The nature of the two phase flow is generally classified based on the particle loading ratio (β). For small values of β it is a sizable assumption to disregard the effect of the particles on the fluid field and simple numerical models based on one-way coupling may be used (Di Giacinto et al., 1982)

In order to classify the nature of flow an analysis was conducted to calculate the value of beta. The average droplet number concentration per cubic meter of fuel gas was computed. The calculation was carried out by combining results from TEM analysis to arrive at an average particle diameter (volume mean diameter) and then relate it to the droplet mean diameter using empirical relations (Wiedmann and Ravichandran, 2001). The precursor atomization rate was then used to get the average number concentration 1.274×10^{12} of droplets entrained per cubic meter of fuel gas and in turn the particle loading ratio of 8.33×10^{-5} . (Calculations attached in the Appendix B)

The regimes of two phase flow are recognized as a function of particle volume fraction. It is known that when particle volume fractions are in the order of $<10^{-3}$ the flow can be considered to be a 'dilute dispersed' two phase flow and a one way coupling method can be used to analyze it (Sommerfeld, 2000).

Having recognized the nature of the two phase flow, the flow through the impactor was simulated using FLUENT 6.2 (Fluent Inc., Lebanon, NH). The discrete phase formulation based on the Lagrangian approach was used.

Simulation description and results

Fluid and particle transport through the impactor was modeled with an Eulerian-Lagrangian framework. The bulk fluid (continuous phase) flow field was solved using the Eulerian approach and then the particle trajectories were calculated using Lagrangian tracking, with the assumption that the particles neither influence the flow field nor each other.

The solved flow was seeded with five hundred particles each of size 1, 2, 3, 4, 5…10 respectively, was tracked through the impactor. A 3D domain of the impactor is shown in Figure 16 while Figure 17 shows the quality of the generated mesh. Figure 18 shows the 3D velocity profiles through the mid-plane of the impactor.

All the droplets in the size range of 1-3 μm passed through the impactor without being collected. 483 of the 4 μm particles, 242 of the 3 μm particles were collected (Table 5). The particle tracks for 1 μm and 10 μm particles are shown in Figure 19 and 20 respectively. An impactor efficiency curve was plotted and an ideal cut-off diameter of 4.8 μm was obtained. This is comparable with the calculated value of 4.5 μm using impactor dimensions (Hinds, 1999). The 4.8 μm is a point of 50% collection and it can be seen that 7 μm is a point of 100% collection.

Summary of Results

Table 6 shows the summary of results from experimental trials. Phase pure monoclinic yttrium oxide particles were synthesized through the flame spray process. 0.65 mol/L precursor solution was used and atomized by the process of ultrasonic atomization. The precursor droplets were passed through an impactor into a pure hydrogen flame using oxygen as a co-flow. Nozzle heating at 130 VA was used. An XRD analysis of the end sample showed all monoclinic particles while a TEM analysis showed a particle size range of 0.350 to 1.2 μm. The process produces around 50 mg of material in an hour. The production rate is slightly lowered due to the use of the impactor.

4. CONCLUSION

Phase controlled yttrium oxide micro and nano particles were successfully synthesized using the technique of flame spray pyrolysis. Ultrasonic atomization was used to feed the precursor droplets into the flame. The effect of flame temperature, flame residence time, precursor concentration and precursor droplet sizes on the size and crystal structure of the product Y_2O_3 particles was investigated. It was found that when FSP was used with precursor concentration of 0.65 mol/L, 1/6" burner with full powered nozzle heating and pure hydrogen flame, monoclinic yttrium oxide was synthesized. The higher flame temperatures and precursor heating support the formation of spherical and unagglomerated monoclinic particles. The fraction of the cubic phase was related to the mean particle diameter. All particles larger than the critical diameter had a cubic structure. An impactor was used to prevent the larger sized droplets from entering the flame. Due to practical difficulties of quantifying the impactor efficiency, a numerical simulation was used to model the flow through the impactor. A one way coupling model was assumed and droplets in the size range of 1-10 μm were tracked. An impactor efficiency curve was plotted which gave a cut-off diameter of 4.8 μm. A study of particle sizes was using the TEM images suggest particle sizes in the range of 0.3 to 1.7 μm.

REFERENCES

Chang, H., Lenggoro, I. W., Okuyama, K. and Kim, T. O. (2004). Continuous Single-Step Fabrication of Nonaggregated, Size-Controlled and Cubic Nanocrystalline Y2o3 : Eu3+ Phosphors Using Flame Spray Pyrolysis. *Japanese Journal of Applied Physics* 43:3535-3539.

Di Giacinto, M., Piva, R. and Sabetta, F. (1982). Two-Way Coupling Effects in Dilute Gas-Particle Flows. *ASME, transactions, Journal of Fluids Engineering* 104:304-312.

Guo, B., Harvey, A., Risbud, S. H. and Kennedy, I. M. (2006). The Formation of Cubic and Monoclinic Y_2o_3 Nanoparticles in Gas-Phase Flame Process. *Philosophical Magazine Letters* 86:457-467.

Guo, B. and Luo, Z. (2007). Y_2O_3 Particles Synthesized in a Flame Process with Size-Dependent Crystal Structure, Texas A&M University, College Station

Hinds, W. C. (1999). *Aerosol Technology: Properties, Behavior and Measurement of Airborne Particles,* 2 ed., Wiley-Interscience, New York.

Ichinose, N., Ozaki , Y., Kashu, S., James, M. and Shields, M. J. (1992). *Superfine Particle Technology*, Springer Verlag, London.

Kruis, F. E., Fissan, H. and Peled, A. (1998). A Review of Nanoparticles in the Gas Phase for Electronic, Optical and Magnetic Applications. *Journal of Aerosol Science* 29:511-535.

Lenggorro, W. and Hata, T. F. I., Lunden, M. M. and Okuyama, K. (2000). An Experimental and Modeling Investigation of Particle Production by Spray Pyrolysis Using a Laminar Flow Aerosol Reactor. *Journal of Material Research*.15:733-743.

McHale, J. M., Auroux, A., Perotta, A. J. and Navrotsky, A. (1997). Surface Energies and Thermodynamic Phase Stability in Nanocrystalline Aluminas. *Science* 277:788-791.

Navrotsky, A., Xu, H., Moloy, E. C. and Welch, M. D. (2003). Thermochemistry of Guest-Free Melanophiogite. *American Mineralogist (Letter)* 88:1612-1614.

Pratsinis, S. E. (1998). Flame Aerosol Synthesis of Ceramic Powders. *Prog. Energy Combust. Sci.* 24:197-219.

Rittner, M. N. (2002). Market Analysis of Nanostructured Materials. *American Ceramic Society* 81:33-36.

Rosner,D.E. (2005). Flame Synthesis of Valuable Nanoparticles: Recent Progress/Current Needs in Areas of Rate Laws, Population Dynamics and Characterization. *Ind. Eng. Chem. Res.* 44:6045-6055.

Sommerfeld, M. (2000). Overview and Fundamentals in *Theoretical and Experimental Modeling of Particulate Flow,* J. M. Buchlin, ed., Von Karman Institute, Brussels, Belgium.

Tok, A. I. Y., Boey, F. Y. C., Du, S. W. and Wong, B. K. (2006). Flame Spray Synthesis of Zro_2 Nano-Particles Using Liquid Precursors. *Materials Science and Engineering* 130:114-119.

Tok , A. I. Y., Boey, F. Y. C., Su, L. T. and Ng, S. H., Flame Synthesis of Nanoparticles, http://www.ntu.edu.sg/MSE/content/research/Rare/default/earth9.asp, (accessed April 19, 2007)

Wiedmann, T. S. and Ravichandran, A. (2001). Ultrasonic Nebulization System for Respiratory Drug Delivery. *Pharmaceutical Development and Technology,* 6:83-89.

Willingham, C. B., Wahl, J. M., Hogan, P. K., Kupferberg, L. C., Wong, T. Y. and De, A. M. (2003). Densification of Nano-Yttria Powders for Ir Window Applications. *Proc. SPIE* 5078:179-188.

APPENDIX A

SAFE OPERATING PROCEDURES

The safe operating procedures include pre-experiment activities, the experimental and the post test activities.

Pre-Experiment Activities

The following activities were carried out as pre-experiment activities.

Gas and Electrical Connections

- It was made sure that all the mass flow controllers (MFCs) are turned off, the gas cylinder main valves are shut off and the heater is turned off.
- The gas lines connections were checked to make sure they were attached to the correct cylinders.
- Connections were made between the desired MFCs and the gas lines from the MFCs to the burner. It was made sure that the gas type and maximum flow rate information in the mass flow control programmer / display (main control box) is correct for every MFC.
- It was verified that the gases are led to the correct inlets of the burner.
- It was made sure that the switch of the variable transformer is at the “OFF” position.
- The heater is connected to the variable transformer.

Burner Cleaning and Precursor Packing

- The initial contamination from the burner was cleaned using brushing, washing and blowing etc. additional care was taken when disconnecting the burner to avoid damage.' wiggling action' was used for successful disassembly.
- A clean beaker is kept ready before the start of experimentation. Chemical was weighed on a weighing paper and then transferred to the beaker for preparation of the precursor solution.
- The precursor solution is then prepared by adding the appropriate measured quantity of distilled water to the measured quantity of precursor in the beaker. (for e.g. 0.026 mol/L solution is prepared by dissolving 1gm of yttrium nitrate hex hydrate in distilled water to make the final solution volume as 100 ml.

Ultrasonic Atomizer: Cleaning and Handling

- The atomizer unit has a stainless steel vessel unit with a thin plastic film underneath. The atomization vessel is specifically kept clean before start of experimentation to avoid contamination.
- The atomizer unit is kept submerged under water for correct operation.
- A syringe pump is used to pump the precursor solution at a constant rate into the vessel.The operation of the syringe pump is checked before usage.It is set at a correct 'volume' and 'rate'. Leaks are also checked between the syringe pump and the vessel.

- **Caution :** ***The mounting of the atomiser with the burner unit is done cautiously to avoid the damage of the thin plastic film and atomiser parts.***

Experiment Activities

The following activities are carried out with the start of the experiment.

- Start of synthesis
- The plastic vessel holding the atomizer was filled with the optimum amount of water to protect the piezo crystal from over-heating during operation.
- The syringe is filled with the precursor solution. We mount the syringe correctly. Make sure the syringe pump is set to a correct 'volume (in ml)' and 'rate in (ml/hr)'.The supply is not started as yet.
- It was made sure that a correct set point is set for nitrogen gas. The purge gas (nitrogen) supply was started and was allowed to run for 30 seconds at a flow rate of 1L/min.
- It was made sure that a correct set point is set for hydrogen gas in the MFC, the supply of hydrogen was then started.
- The nozzle heater was then turned on and set it to a correct voltage. It was then checked to see if the thermocouple is hooked up and correctly placed.
- After a wait period of 30 seconds the purge gas supply was stopped.
- The front end of the 'synthesis chamber' was then closed with a plexi-glass cover, and the flame is started with a lighter.
- The oxygen gas supply was started to notice a stable bright flame.
- A steady temperature is reached as shown by the temperature indicator after approximately ten to fifteen minutes.
- After a steady temperature is reached, some precursor solution was pushed through the syringe into the atomization vessel.

- The atomizer is then started.
- After noticing a steady aerosol streak, the supply of precursor to the atomization vessel was started.
- The vacuum pump is also started to start the process of particle collection.

Sampling

- A filtration device was used to undertake the process of sampling. Care was taken in positioning the sapling tube so that no overheating occurs.

Shutdown

The following 'shutdown' procedure was followed**:**

- When the aerosol streak disappears (suggesting that the entire quantity of precursor in the atomization vessel has been used, syringe pump has pushed out the preset volume) it is time to stop the experiment.
- The vacuum pump is turned off first.
- Next turn off all gases by pressing "OFF" "ALL" on the mass flow controller. Then TURN OFF THE INDIVIDUAL CHANNELS.
- Turn off the oxygen gas first.
- Turn on the nitrogen gas supply next.
- Turn off the hydrogen gas next, wait for 30 seconds until the flame completely disappears.
- Shut the main valve of each compressed gas cylinder.
- Shut off the nozzle heater and atomizer.

Sample retrieval

- The filter holder was then removed by disconnecting the ¼" stainless steel tube that is attached to the back of the filter holder from the vacuum line. Special care was taken while handling the filter holder because of the high temperature of the filter holder, the burner and the heater. The filter holder is cooled to a safe temperature before retrieving the filter.
- A Petri dish was made ready for storing the filter sample.
- The filter holder while maintaining its upright position (filter facing up) was removed. The filter is then exposed. The filter was then picked up with a pair of sharp tweezers. Special care is taken to avoid breaking or cracking the filter. The filter sample is then put into the Petri dish with the sample side facing up.

Post Test Activities

- It was made sure that the gas cylinders are shut off.
- It was made sure that all spills and debris has been cleaned.

Analysis of Samples

The following techniques of analysis were used:

- X-ray Diffraction analysis (XRD): The x-ray diffraction technique was used to analyze the chemical composition and the phase of the synthesized powder samples. The Bragg/Brentano powder diffractometer and the high resolution powder diffractometer were alternatively used for this purpose. The high resolution powder diffractometer (The D8 VARIO) has a sealed X-ray source (Cu) in the standard

vertical θ-2θ geometry. A Germanium incident beam monochromator is used to produce $K\alpha_2$ free radiation. A linear PSD detector is employed for data collection. The Bragg/Brentano powder diffractometer has standard powder diffractometer with a sealed X-ray source (Cu) in the vertical 2 theta geometry.

- Transmission Electron Microscopy analysis (TEM) was used to analyze the crystal structure and size and morphology of the synthesized samples. A JEOL 2010 operated at 200 kV was used for the TEM analysis.

APPENDIX B

CALCULATIONS AND SIMULATION RESULTS

1.Particle Loading Ratio (β) calculation

Volume of a droplet = $\frac{\pi\left(d_p\right)^3}{6}$

Average droplet diameter (micrometer) D_d = Average Y_2O_3 diameter (micrometer) D_p X Conversion factor f .

$$D_p = f \times D_d$$

Where D_p = Particle diameter

D_d = Precursor droplet diameter

f = Conversion factor

Using a 0.65 mol/L concentration of precursor we have f = 0.3

(Using a 0.65 mol/L solution, we have concentration of 1.25 g/cc,

starting with 1μm droplet of 5.236 e-19 m^3 volume and 6.545 e-16 Kg., mass.

25% of the droplet mass will be Y $(NO_3)_3$ which is 1.636e-16 Kg.

Moles of Yttrium = $\frac{\text{Mass of yttrium nitrate (kg.)}}{\text{Molecular mass of Yttrium nitrate (kg. /mole)}}$

= 5.972 e-19 moles of Yttrium

Now 2 moles of Yttrium gives one mole of yttrium oxide therefore 5.972 e-19 moles of

Yttrium gives 2.986e-19 moles of yttrium oxide (6.688e-17 kg of Yttrium oxide)

The density of Yttrium oxide is 5030 kg/m^3 , volume of yttrium oxide will be 1.3296e-20

Therefore $\frac{\pi d_p^{\,3}}{6} = 1.3296e-20$

d_p = 0.3 μm)

From the TEM images the average particle size (equivalent volume diameter) is found to be 1.5 μm

Avg. Equivalent volume droplet diameter = 5 μm

Average Volume of droplets= $\frac{\pi \times (5e-6)^3}{6} = 6.54 \times 10^{-17} m^3$

Droplet number flow rate = liquid atomization rate/ Average volume of droplets

$= 2.124 \times 10^7$ / sec

Average Number of droplets/ volume of fuel gas

$= 1.274 \times 10^{12}$ number/ m^3

β (Particle loading ratio) = 8.33e-5

2. FLUENT Simulation Results for Particle Tracking Through the Impactor.

FLUENT
Version: 3ddp, segregated, lam (3d, double precision, segregated, laminar)
Release: 6.2.16
Title:

Models

Model	Settings
Space	3D
Time	Steady
Viscous	Laminar
Heat Transfer	Disabled
Solidification and Melting	Disabled
Species Transport	Disabled
Coupled Dispersed Phase	Disabled
Pollutants	Disabled
Soot	Disabled

Boundary Conditions

Zones

Name	Id	Type
Fluid	2	Fluid
Inlet	7	mass-flow-inlet
opening	4	outlet-vent
Wall	3	Wall
impaction plate	5	Wall
outlet	6	Outflow
default-interior	9	Interior

Boundary Conditions (fluid)

Material Name	hydrogen
Motion Type	0
X-Velocity Of Zone	0
Y-Velocity Of Zone	0
Z-Velocity Of Zone	0
Rotation speed	0
X-Origin of Rotation-Axis	0
Y-Origin of Rotation-Axis	0
Z-Origin of Rotation-Axis	0
X-Component of Rotation-Axis	0
Y-Component of Rotation-Axis	0
Z-Component of Rotation-Axis	1
Deactivated Thread	no
Porous zone?	no
Conical porous zone?	no
X-Component of Direction-1 Vector	1
Y-Component of Direction-1 Vector	0
Z-Component of Direction-1 Vector	0
X-Component of Direction-2 Vector	0
Y-Component of Direction-2 Vector	1
Z-Component of Direction-2 Vector	0
X-Coordinate of Point on Cone Axis	1
Y-Coordinate of Point on Cone Axis	0
Z-Coordinate of Point on Cone Axis	0
Half Angle of Cone Relative to its Axis	0
Direction-1 Viscous Resistance	0
Direction-2 Viscous Resistance	0
Direction-3 Viscous Resistance	0
Direction-1 Inertial Resistance	0
Direction-2 Inertial Resistance	0
Direction-3 Inertial Resistance	0
C0 Coefficient for Power-Law	0
C1 Coefficient for Power-Law	0
Porosity	1

Inlet Conditions

Condition	Value
Mass Flow Specification Method	0
Mass Flow-Rate	1.37E-06
Mass Flux	1
Average Mass Flux	1
Upstream Torque Integral	1
Upstream Total Enthalpy Integral	1
Supersonic/Initial Gauge Pressure	0
Direction Specification Method	1
Reference Frame	0
Coordinate System	0
X-Component of Flow Direction	1
Y-Component of Flow Direction	0
Z-Component of Flow Direction	0
X-Component of Axis Direction	1
Y-Component of Axis Direction	0
Z-Component of Axis Direction	0
X-Coordinate of Axis Origin	0
Y-Coordinate of Axis Origin	0
Z-Coordinate of Axis Origin	0
Discrete Phase BC Type	4
Discrete Phase BC Function	none
Is zone used in mixing-plane model?	no

Opening Conditions

Condition	Value
Gauge Pressure	0
Radial Equilibrium Pressure Distribution	no
Backflow Direction Specification Method	1.00E+00
Coordinate System	0
X-Component of Flow Direction	1
Y-Component of Flow Direction	0
Z-Component of Flow Direction	0
X-Component of Axis Direction	1
Y-Component of Axis Direction	0
Z-Component of Axis Direction	0
X-Coordinate of Axis Origin	0
Y-Coordinate of Axis Origin	0
Z-Coordinate of Axis Origin	0
Discrete Phase BC Type	4
Discrete Phase BC Function	none
Is zone used in mixing-plane model?	no
Specify targeted mass-flow rate	no
Targeted mass-flow	1

Wall

Enable shell conduction?	no
Wall Motion	0
Shear Boundary Condition	0
Define wall motion relative to adjacent cell zone?	yes
Apply a rotational velocity to this wall?	no
Velocity Magnitude	0
X-Component of Wall Translation	1
Y-Component of Wall Translation	0
Z-Component of Wall Translation	0
Define wall velocity components?	no
X-Component of Wall Translation	0
Y-Component of Wall Translation	0
Z-Component of Wall Translation	0
Discrete Phase BC Type	3
Normal	

Wall Continued…

Rotation Speed	0
X-Position of Rotation-Axis Origin	0
Y-Position of Rotation-Axis Origin	0
Z-Position of Rotation-Axis Origin	0
X-Component of Rotation-Axis Direction	0.00E+00
Y-Component of Rotation-Axis Direction	0
Z-Component of Rotation-Axis Direction	1
X-component of shear stress	0
Y-component of shear stress	0
Z-component of shear stress	0
Specularity Coefficient	0

Outlet Conditions

Condition	Value
Flow rate weighting	1
Discrete Phase BC Type	4
Discrete Phase BC Function	none

Equation	Solved
Flow	Yes

Relaxation

Variable	Relaxation Factor
Pressure	0.30000001
Density	1
Body Forces	1
Momentum	0.69999999

Linear Solver

	Solver	Termination	Residual Reduction
Variable	Type	Criterion	Tolerance
Pressure	V-Cycle	0.1	
X-Momentum	Flexible	0.1	0.7
Y-Momentum	Flexible	0.1	0.7
Z-Momentum	Flexible	0.1	0.7

Discretization Scheme

Variable	Scheme
Pressure	Standard
Momentum	Second Order Upwind

Solution Limits

Quantity	Limit
Minimum Absolute Pressure	1
Maximum Absolute Pressure	5e+10
Minimum Temperature	1
Maximum Temperature	5000

Material: water-liquid (inert-particle)

Property	Units	Method
Density	kg/m3	constant
Cp (Specific Heat)	j/kg-k	constant
Thermal Conductivity	w/m-k	constant

Material: hydrogen (fluid)

Property	Units	Method	Value(s)
Density	kg/m3	constant	0.081890002
Cp (Specific Heat)	j/kg-k	constant	14283
Thermal Conductivity	w/m-k	constant	0.1672
Viscosity	kg/m-s	constant	8.4109e-06
Molecular Weight	kg/kg mol	constant	2.01594
L-J Characteristic Length	Angstrom	constant	2.92
L-J Energy Parameter	K	constant	38
Thermal Expansion Coefficient	1/K	constant	0

Material: air (fluid)

Property	Units	Method	Value(s)
Density	kg/m3	constant	1.225
Cp (Specific Heat)	j/kg-k	constant	1006.43
Thermal Conductivity	w/m-k	constant	0.0242
Viscosity	kg/m-s	constant	1.7894e-4
Molecular Weight	kg/kg mol	constant	28.966
L-J Characteristic Length	Angstrom	constant	3.711
L-J Energy Parameter	K	constant	78.6
Thermal Expansion Coefficient	1/K	constant	0

APPENDIX C

TABLES AND FIGURES

Table 1. Bill of Materials

S. No.	Description	Bought /Manufactured
1	Nitrogen/Argon Diluents tank	B
2	Oxygen Tank	B
3	Fuel(H_2,CH_4)tank	B
4	Copper Tubing	B
5	Gas Regulator	B
6	Mass flow meter	B
7	AC supply	-
8	Stainless steel tube	B
9	Exhaust duct	B
10	Thermocouple	B
11	Co-flow Burner	M
12	Variable Transformer	B
13	Filter holder	B
14	Filters	B
15	Vacuum pump	B
16	Temperature readout	B
17	Swagelok tube fittings	B
18	Copper tubing	B

Table 2. Estimated Adiabatic temperature of $H_2/O_2/H_2O$ (H_2O as a liquid in starting fuel gas) flames

H_2O/ H_2 molar ratio	0	0.1	0.2	0.3
Adiabatic Temperature (K)	3079	3027	2968	2854

Table 3. Particle size distribution before using an impactor (Yttria particles synthesized by flame spray pyrolysis at H_2 at 1slm and O_2 at 5 slm, 0.65 mol/L concentration, full power nozzle heating)

Particle Size Range (in micrometers)	Number Frequency	Number Fraction
0.200-0.300	0	0
0.300-0.400	0	0
0.400-0.500	0	0
0.500-0.600	2	0.013986
0.600-0.700	16	0.111888
0.700-0.800	14	0.097902
0.800-0.900	36	0.251748
0.900-1.000	30	0.20979
1.000-1.100	17	0.118881
1.100-1.200	5	0.034965
1.200-1.300	6	0.041958
1.300-1.400	9	0.062937
1.400-1.500	1	0.006993
1.500-1.600	1	0.006993
1.600-1.700	3	0.020979
1.700-1.800	0	0
1.800-1.900	2	0.013986
1.900-2.000	1	0.006993
Total Particles measured using TEM	143	

Table 4. Particle size distribution after using an impactor (Yttria particles synthesized by flame spray pyrolysis at H_2 at 1slm and O_2 at 5 slm, 0.65 mol/L concentration, full power nozzle heating)

Particle Size Range (in micrometers)	Number Frequency	Number Fraction
0.200-0.300	0	0
0.300-0.400	8	0.038095
0.400-0.500	19	0.090476
0.500-0.600	50	0.238095
0.600-0.700	63	0.3
0.700-0.800	43	0.204762
0.800-0.900	15	0.071429
0.900-1.000	4	0.019048
1.000-1.100	4	0.019048
1.100-1.200	4	0.019048
1.200-1.300	0	0
1.300-1.400	0	0
1.400-1.500	0	0
1.500-1.600	0	0
1.600-1.700	0	0
1.700-1.800	0	0
1.800-1.900	0	0
1.900-2.000	0	0
Total Particles measured using TEM	210	

Table 5. Simulation Results

Droplet Diameter	Particles introduced in flow stream	Stk Number	Penetrated Particles	Collected by the impactor	Collection Efficiency
1.00E-06	500	0.011248	500	0	0
2.00E-06	500	0.044992	500	0	0
3.00E-06	500	0.101232	500	0	0
4.00E-06	500	0.179968	483	17	0.034
5.00E-06	500	0.281199	242	258	0.516
6.00E-06	500	0.404927	88	412	0.824
7.00E-06	500	0.551151	0	500	1
8.00E-06	500	0.71987	0	500	1
9.00E-06	500	0.911086	0	500	1
1.00E-05	500	1.124798	0	500	1

Table 6. Summary of experimental results (*as the ratio of the height of the cubic peak at 2-theta 29.15 degrees to that of the monoclinic peak at 2-theta 28.587 degrees)

Burner Flow Arrangement (outward from center)	Y(NO3)3 solution droplets+H2 (N2 purge) - O2	Y(NO3)3 solution droplets+H2 (N2 purge) - O2	Y(NO3)3 solution droplets+H2 (N2 purge) - O2	Y(NO3)3 solution droplets+H2 (N2 purge) - O2	Y(NO3)3 solution droplets+H2 (N2 purge) - O2	Y(NO3)3 solution droplets+H2 (N2 purge) - O2	Y(NO3)3 solution droplets+H2 (N2 purge) - O2
Y(NO3)3.6H2O Concentration (mol/L)	0.26	0.26	0.65	0.26	0.026	0.65	0.65
H_2 (SLM)	1.5	1.5	1.5	1.5	1.5	1	1
O_2 (SLM)	10	10	10	7	5	5	5
N_2 (SLM)	1	1	1	1	1	1	1
Heating Voltage (VA)	60	60	60	130	130	130	130
Sampling Time (min)	60	60	60	60	60	60	60
Burner ID (mm)	3	3	8.5	3	3	3	3
Flame Characteristic	Bright pinkish flame	Bright pinkish flame.	Bright pinkish flame	Bright pinkish flame	Bright pinkish flame	Bright pinkish flame	Bright pinkish flame
Notes	-low precursor conc. -No pre heating	-Low precursor conc. -Nozzle heating	-Moderate precursor conc. -Nozzle heating	- Low precursor conc. -Full power nozzle heating	-Very low precursor conc. - Full power nozzle heating	-Moderate precursor conc. -Full power nozzle heating	-Moderate precursor conc. Full power nozzle heating - droplet size control using a round jet impactor
cubic to monoclinic ratio*	2.0	0.9	0.6	0.5	Almost zero	0.7	Phase pure monoclinic

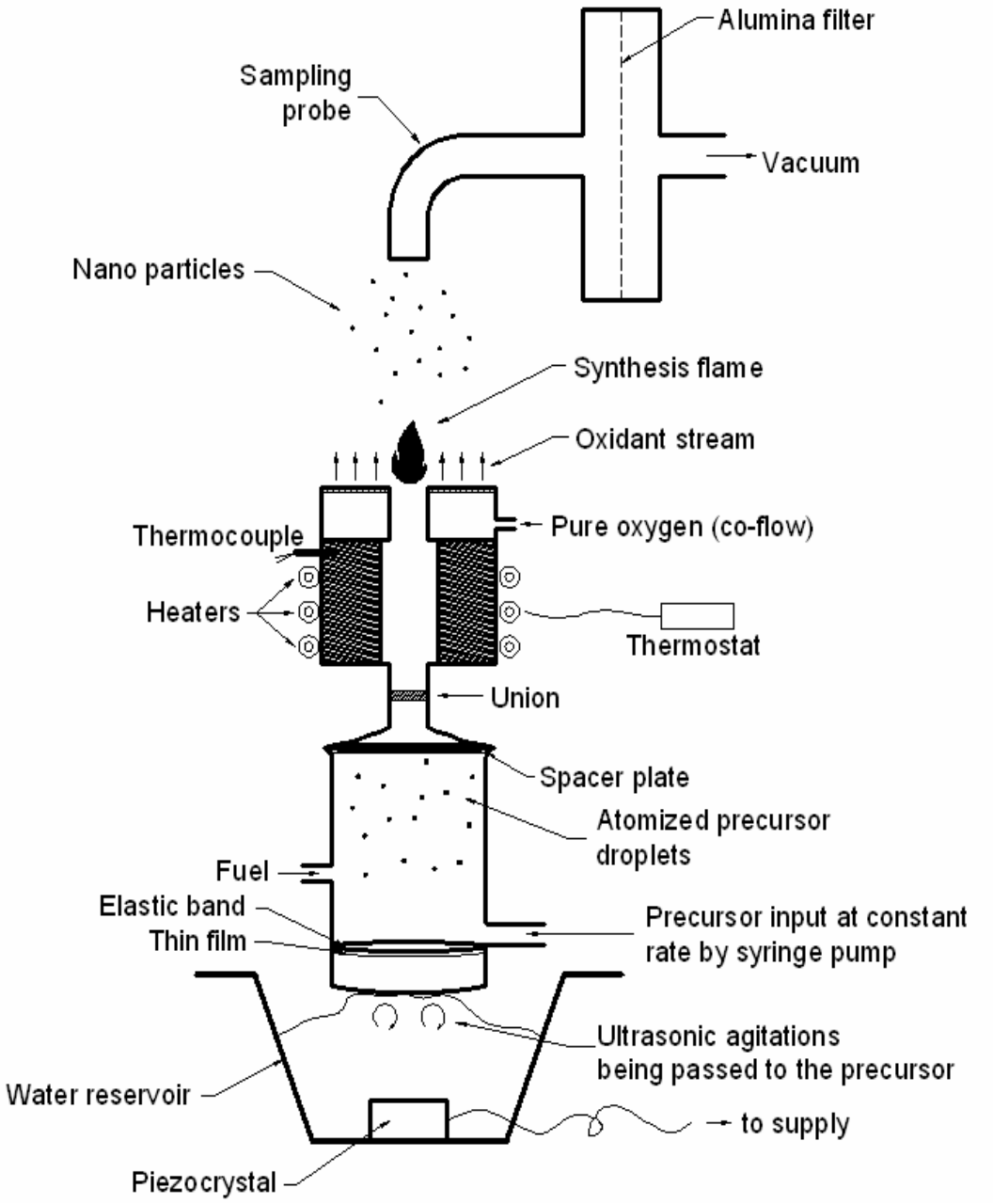

Figure 1. Schematic showing the flame spray pyrolysis set-up

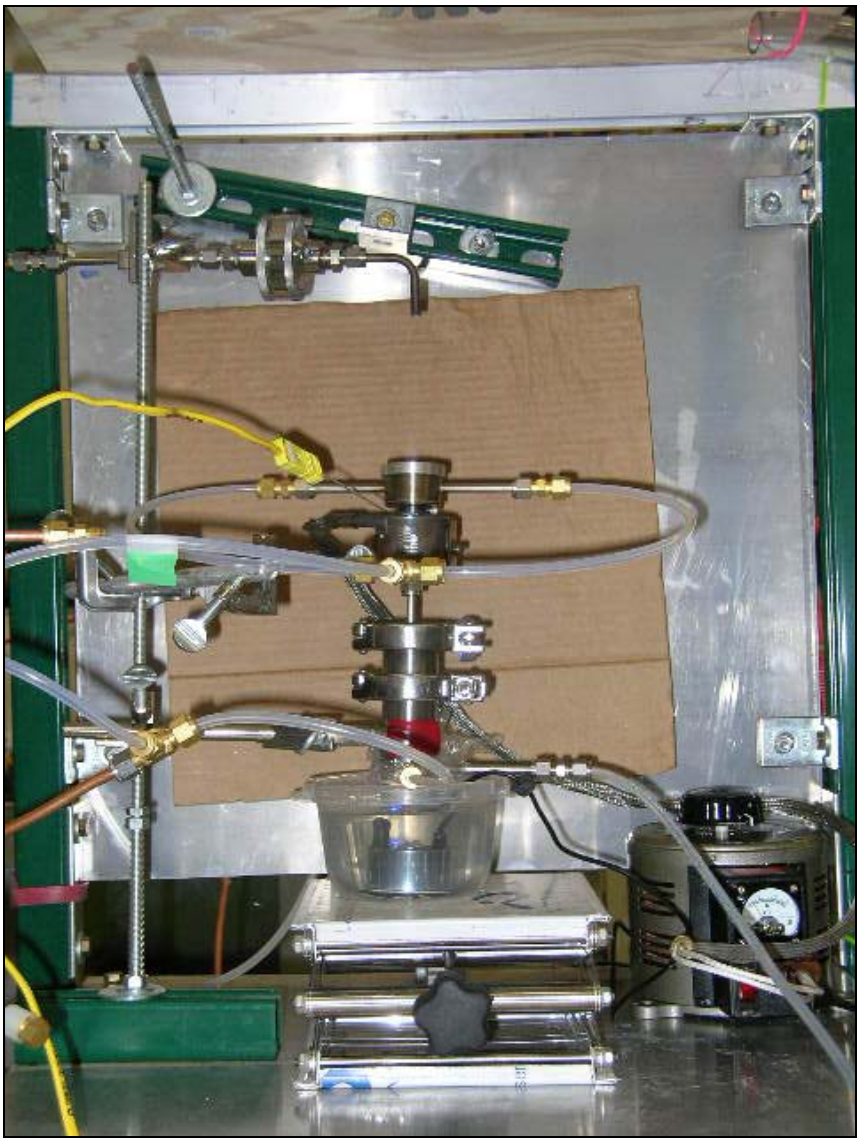

Figure 2. Photograph showing the synthesis chamber set-up

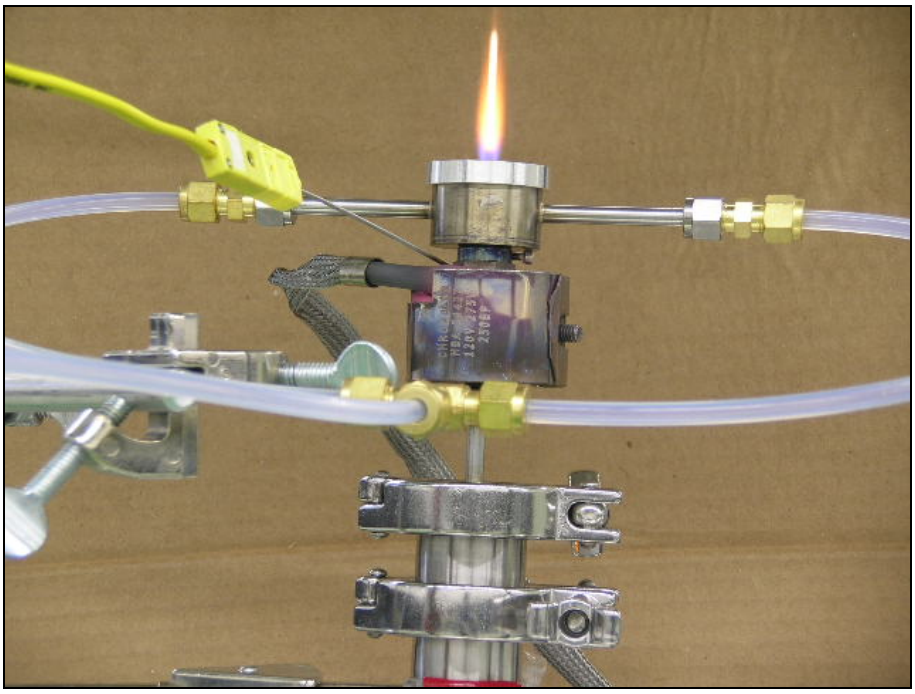

Figure 3. Photograph showing the co-flow burner and the synthesis flame

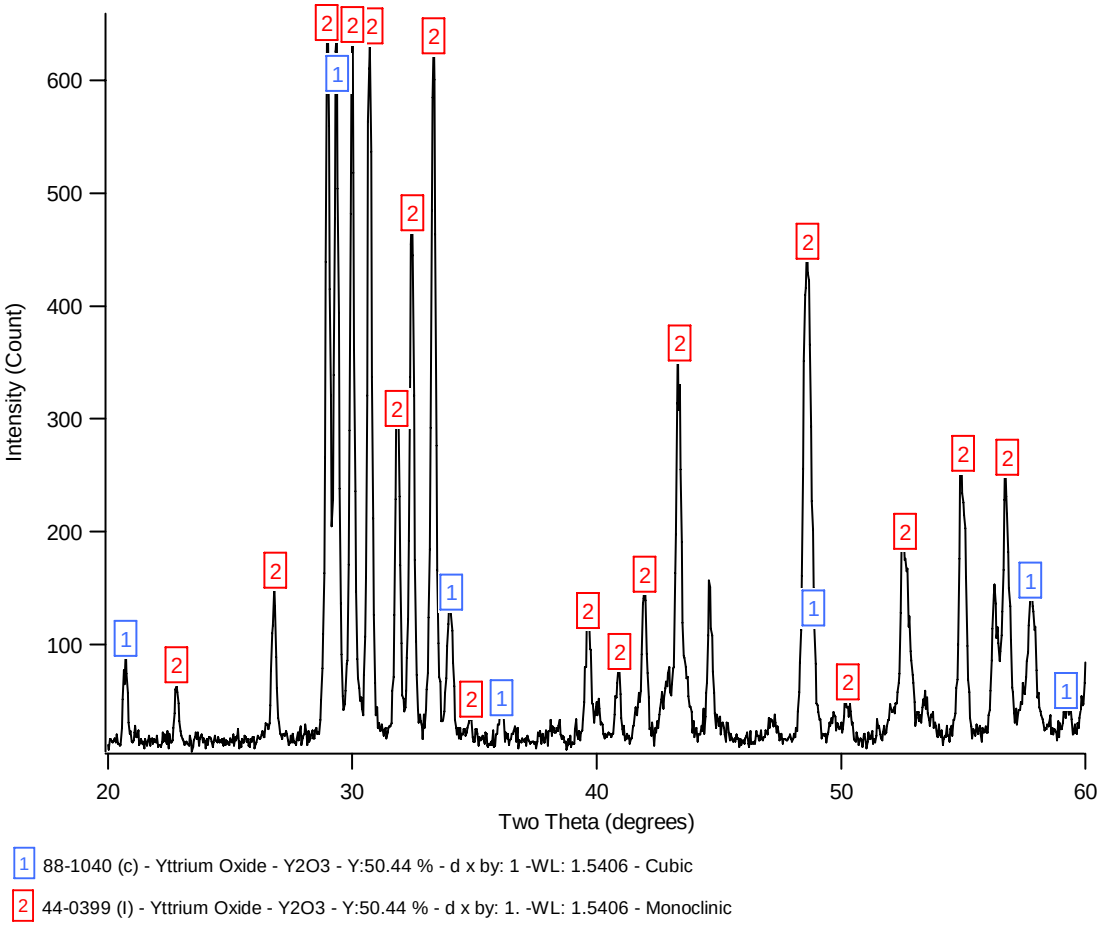

Figure 4. Representative XRD result showing cubic and monoclinic Yttria mixture

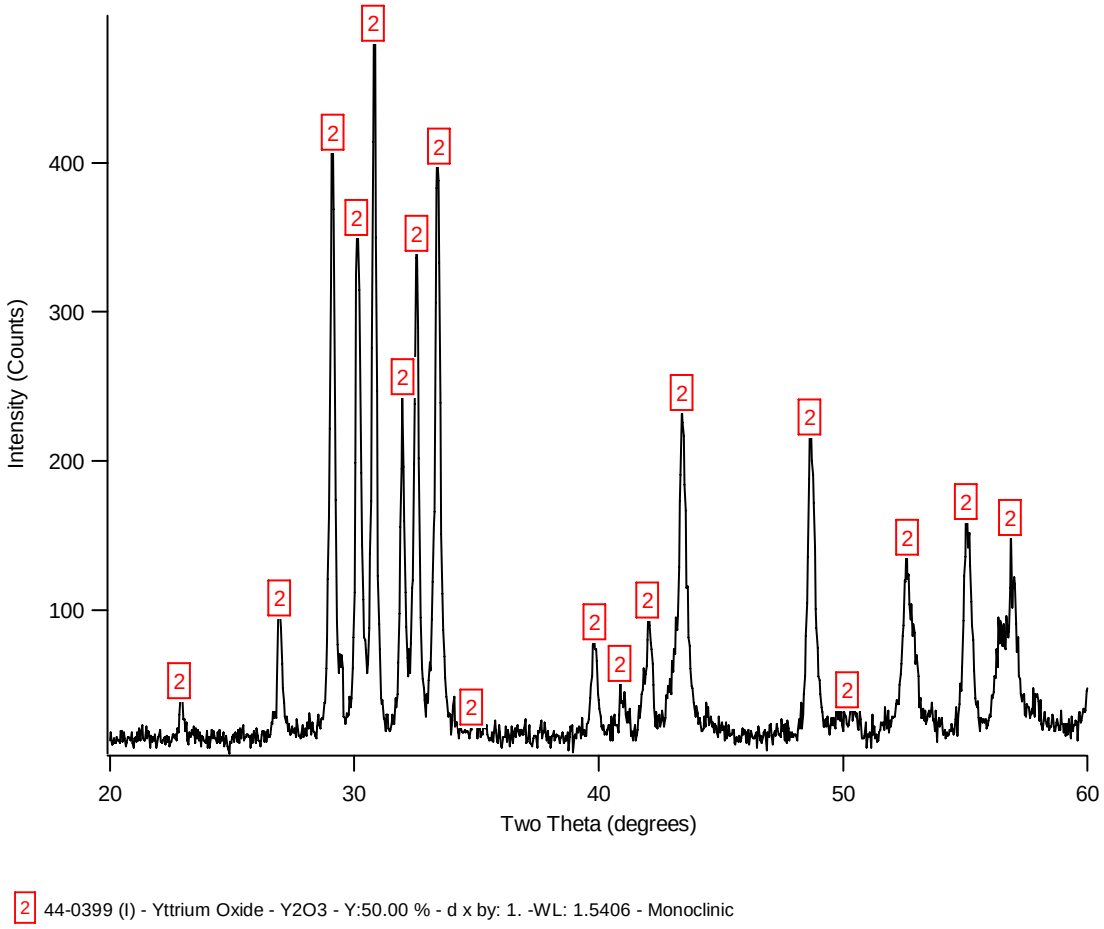

Figure 5. XRD result showing pure monoclinic Yttria sample

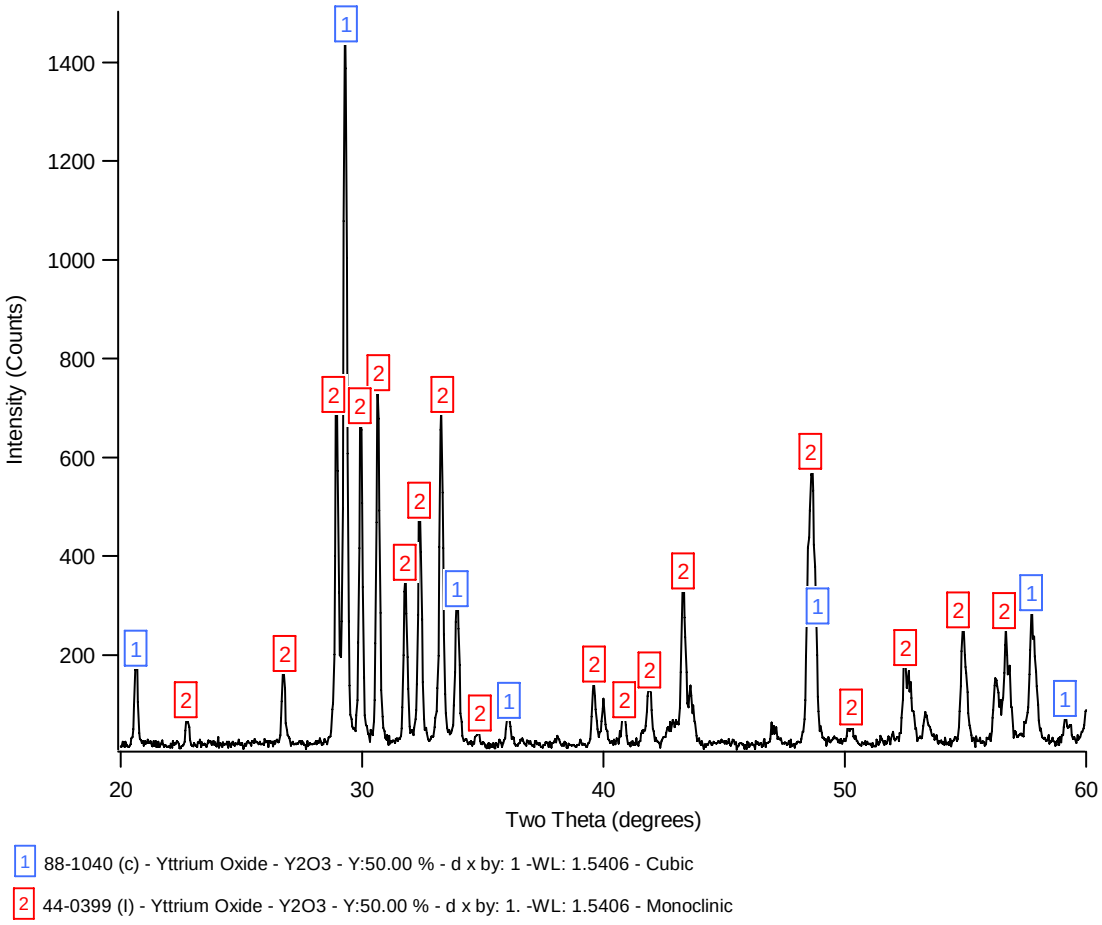

Figure 6. XRD result (No pre-heating, 0.26 mol/L concentration, 1.6 mm burner)

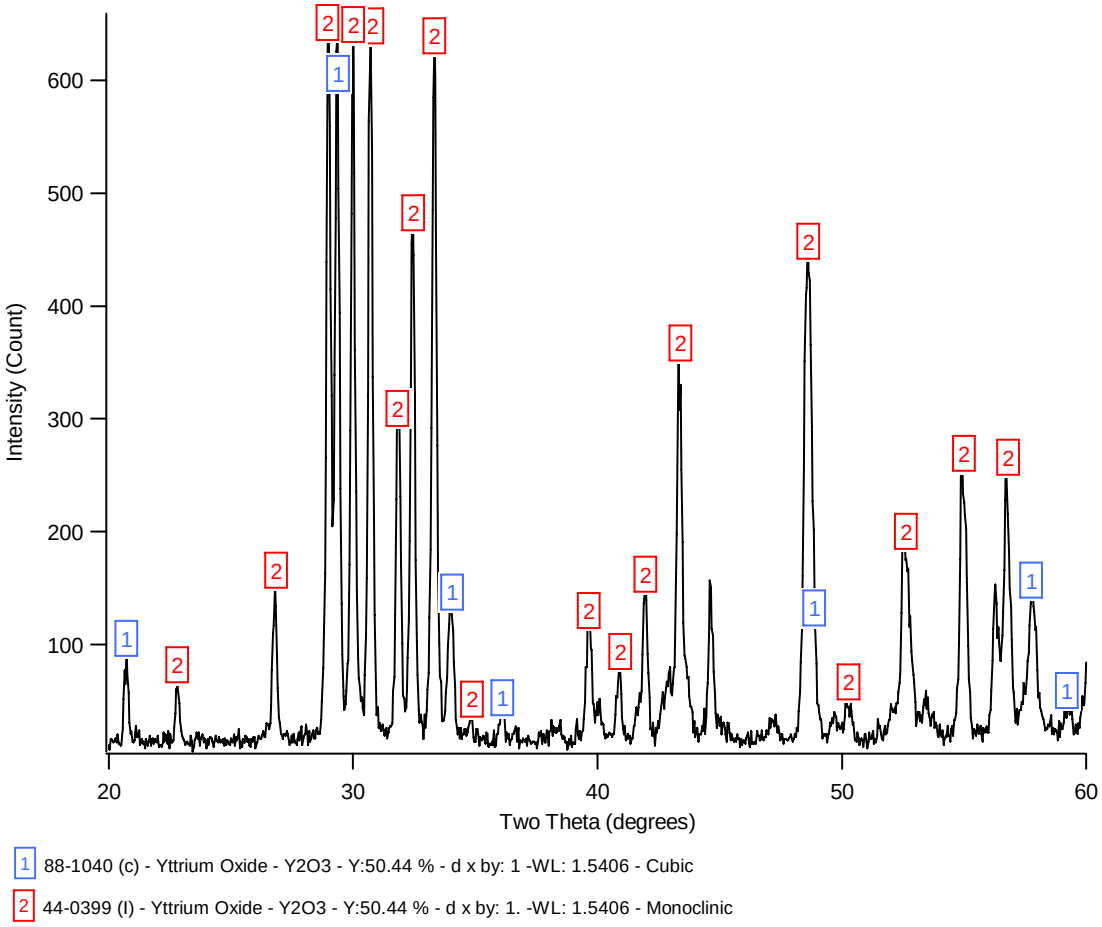

Figure 7. XRD result (60 VA pre-heating, 0.26 mol/L concentration, 1.6 mm burner)

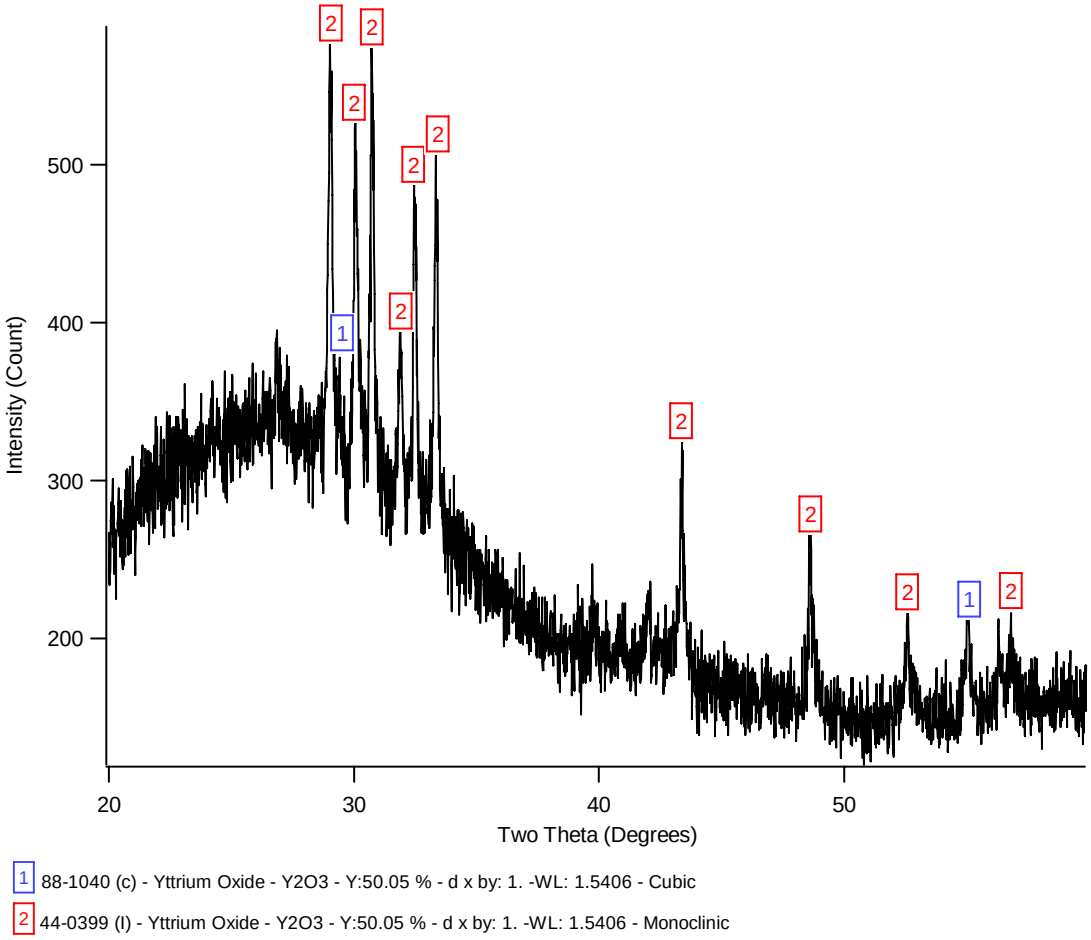

Figure 8. XRD result (full power pre-heating, 0.65 mol/L concentration, 1.6 mm burner)

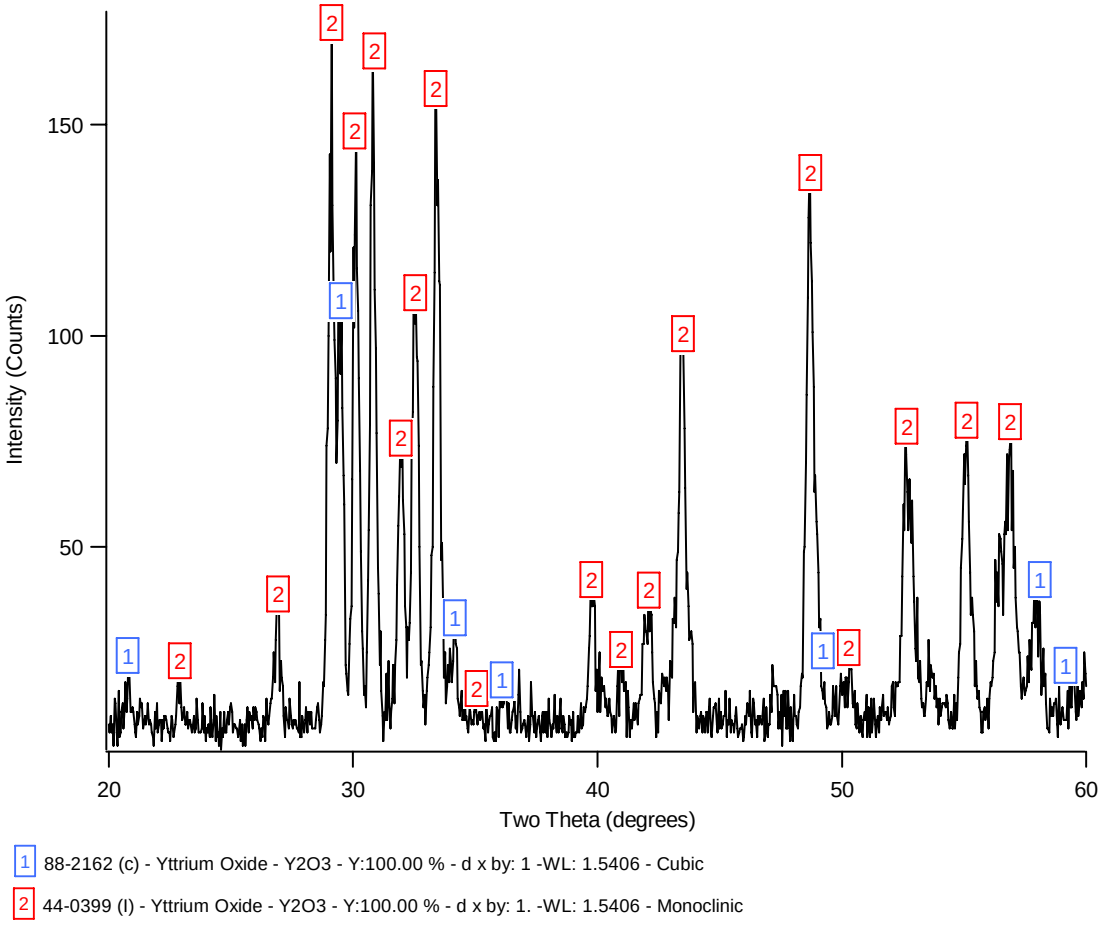

Figure 9. XRD result (9.5 mm burner, 0.65 mol/L concentration, full pre-heating)

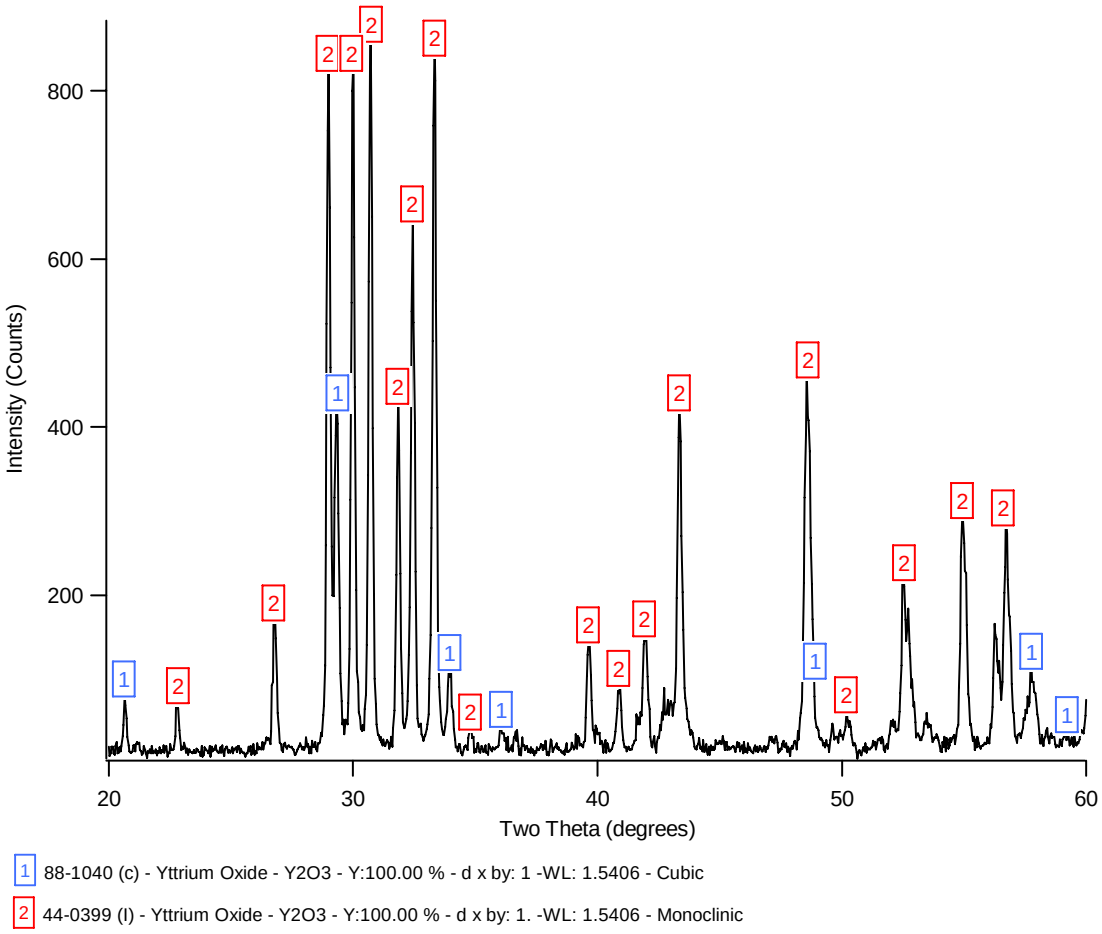

Figure 10. XRD result (Full pre-heating, 0.26 mol/L concentration, 1.6 mm burner)

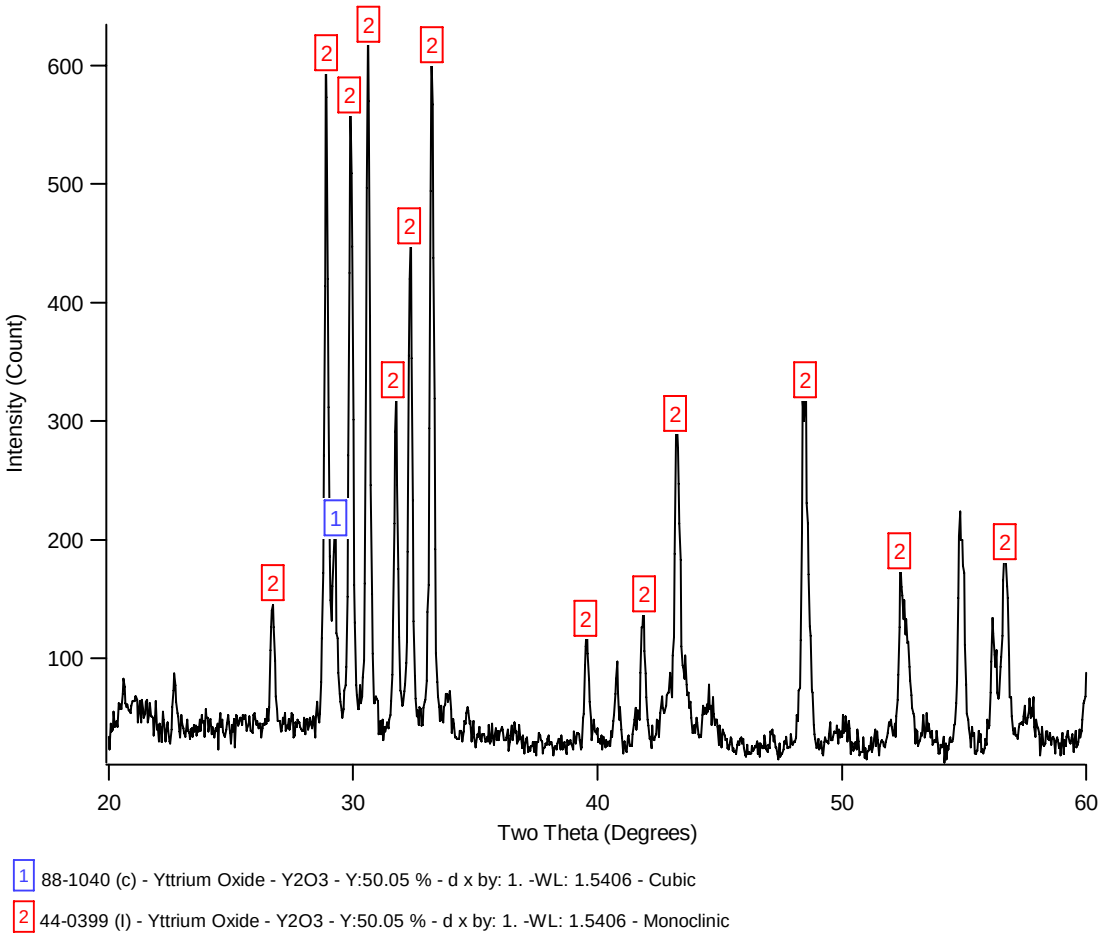

Figure 11. XRD result (Full power pre-heating, 0.026 mol/L concentration, 1.6 mm burner)

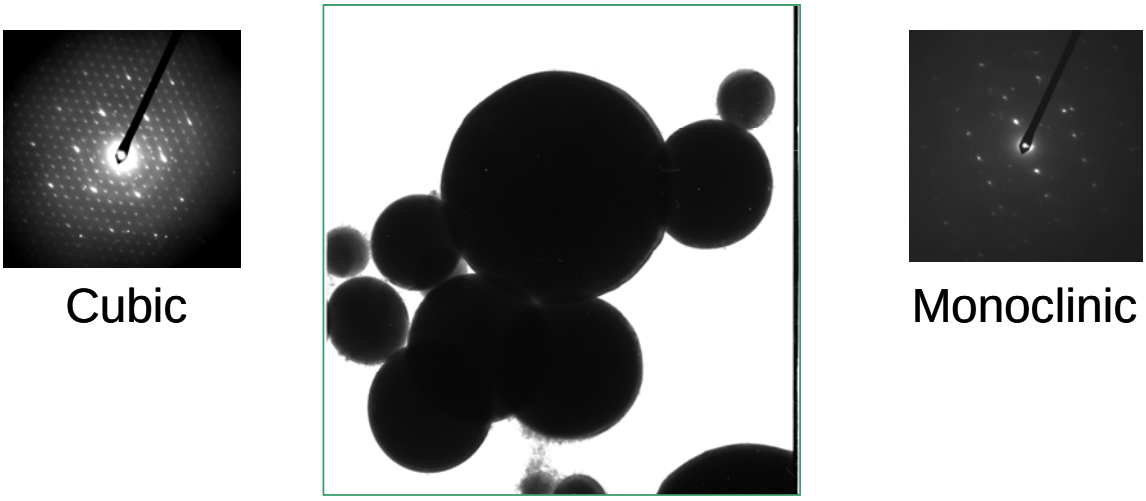

Figure 12. TEM images showing measured particle size effect for Y_2O_3

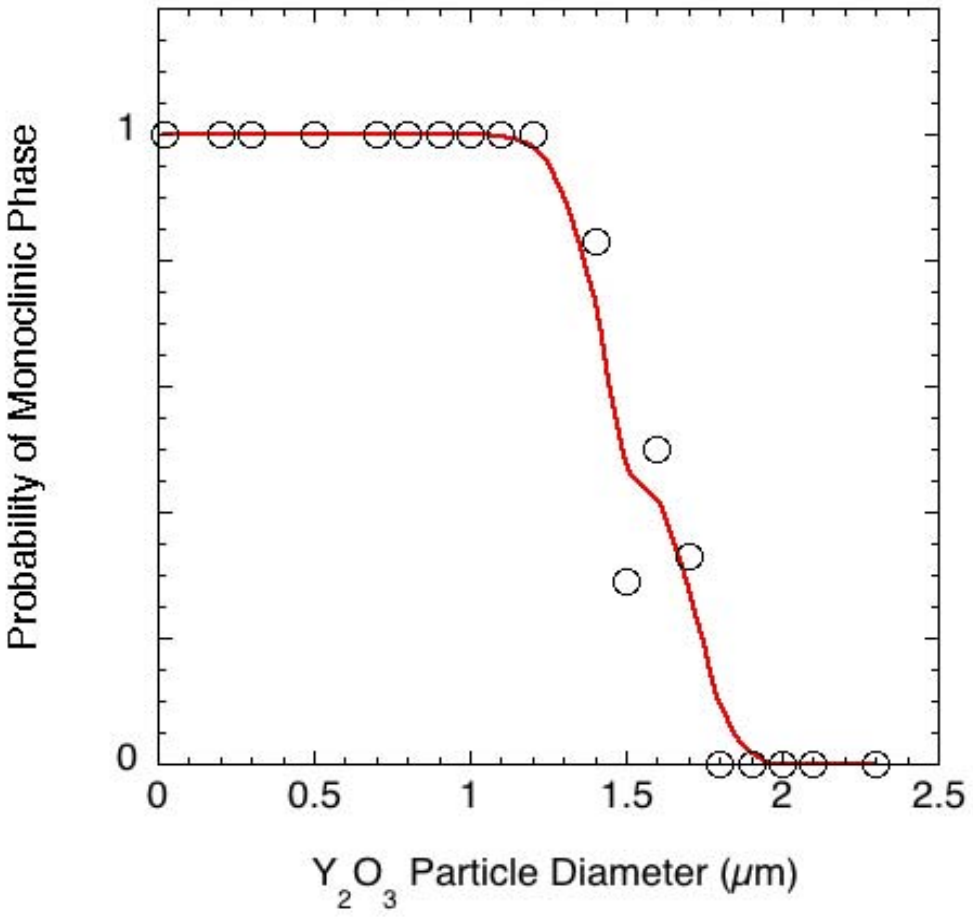

Figure 13. Graph showing size effect (Results from measurement for over 50 individual particles obtained using TEM and SAED)

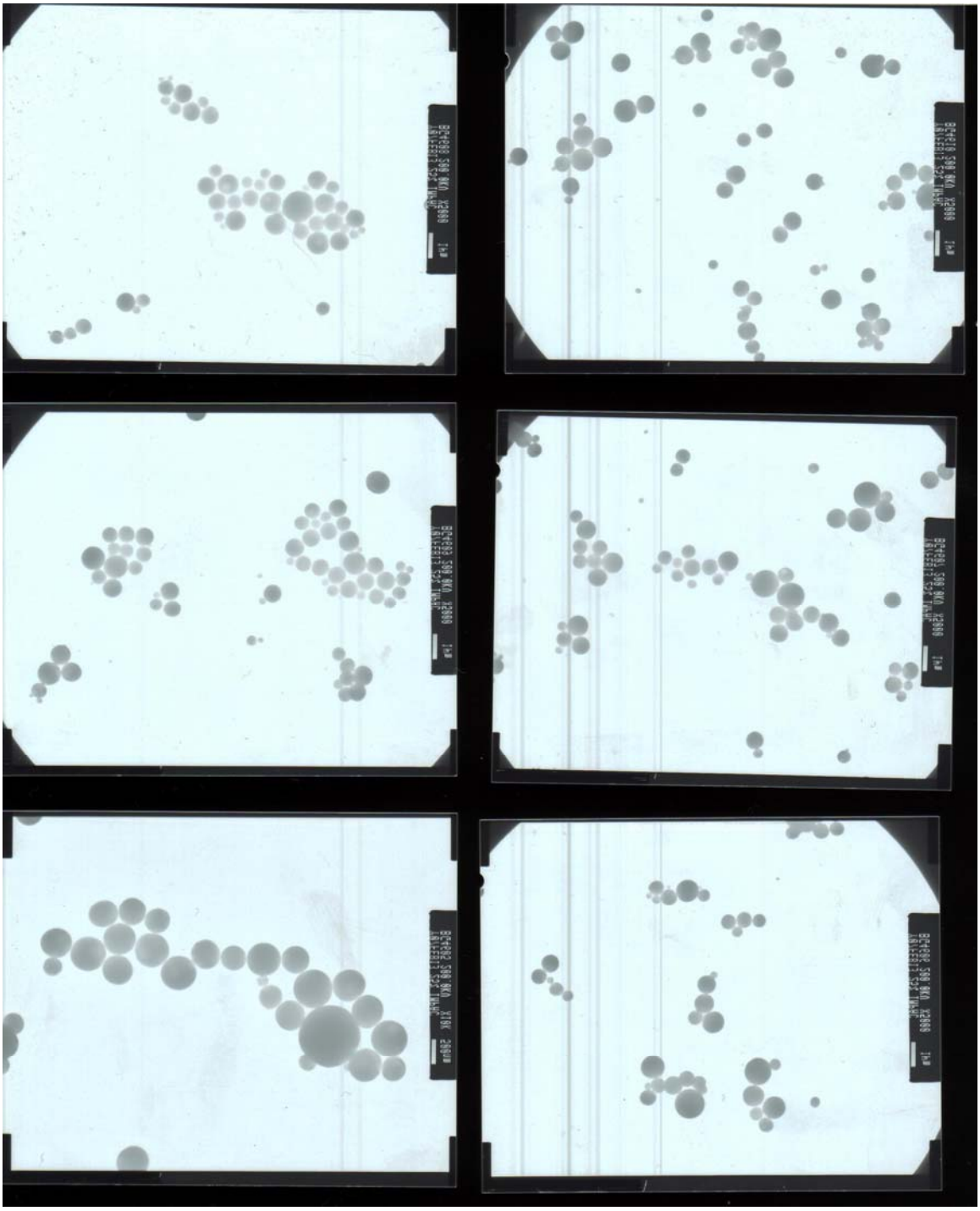

Figure 14. TEM image showing particle size distribution

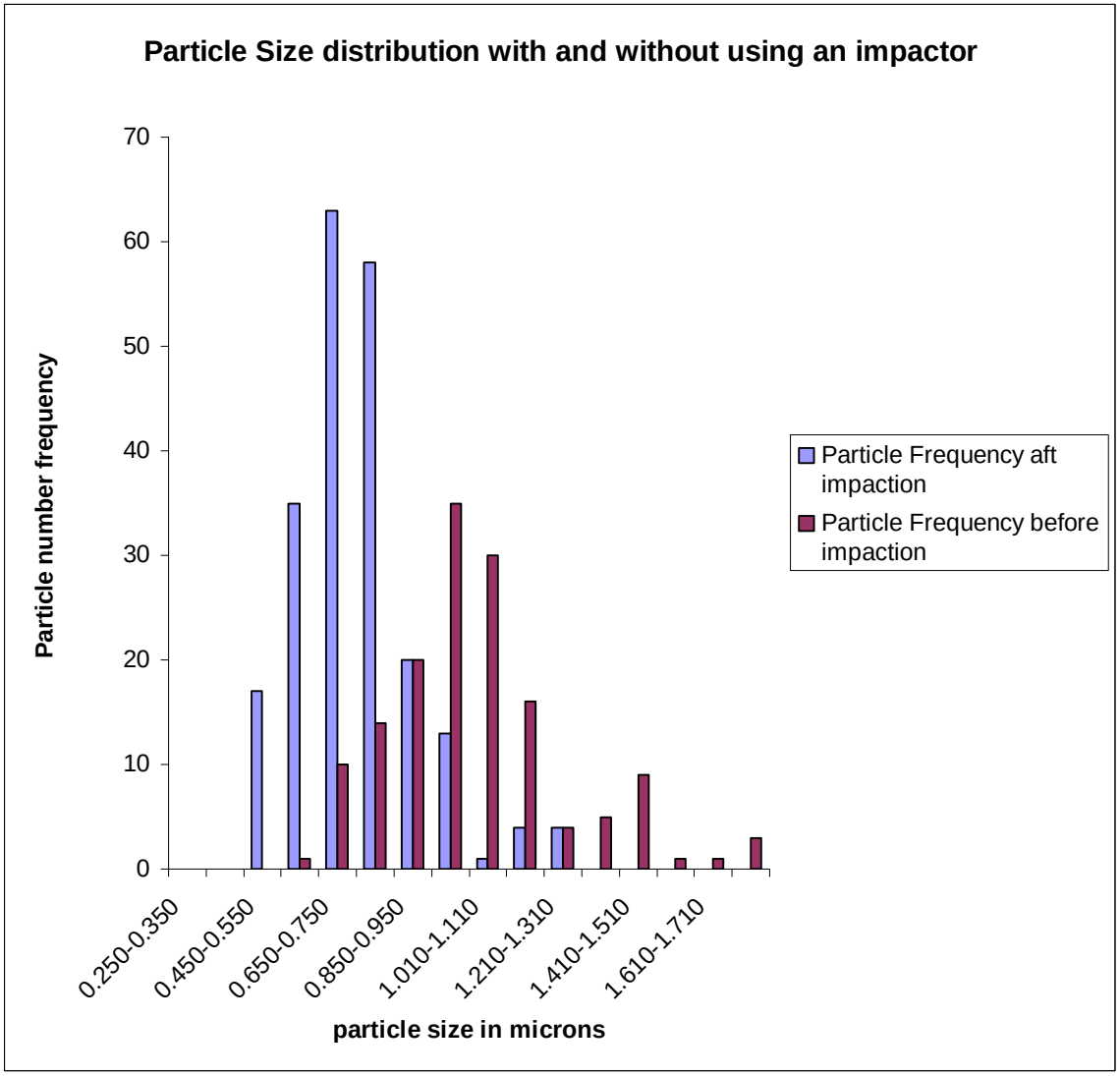

Figure 15. Histogram showing particle size distribution with and without using an impactor

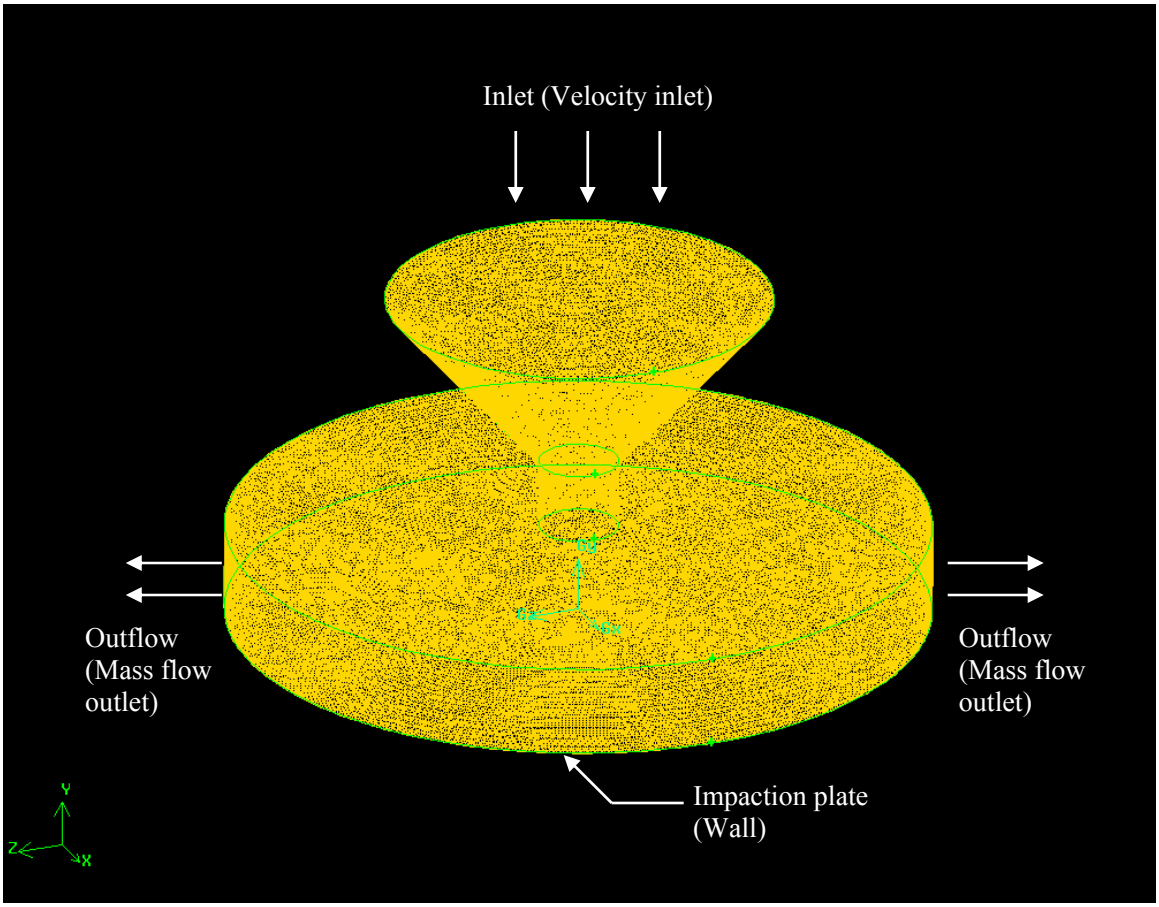

Figure 16. 3D domain of the impactor (mesh image from gambit)

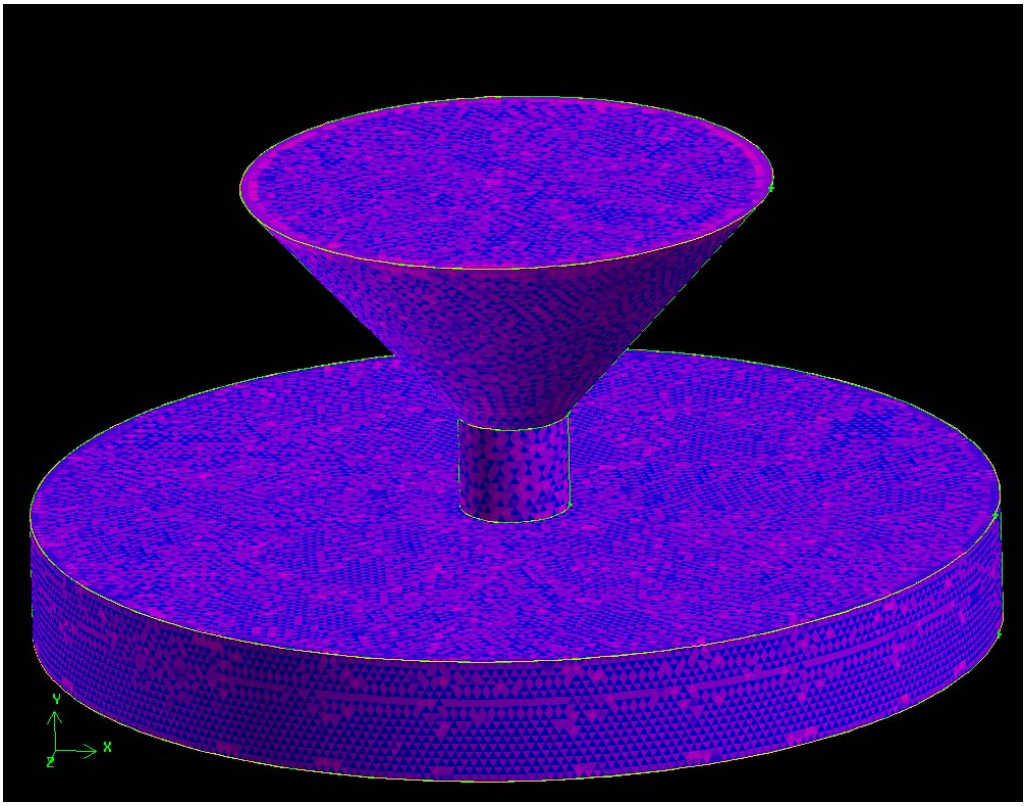

Figure 17. Image from Gambit showing mesh quality

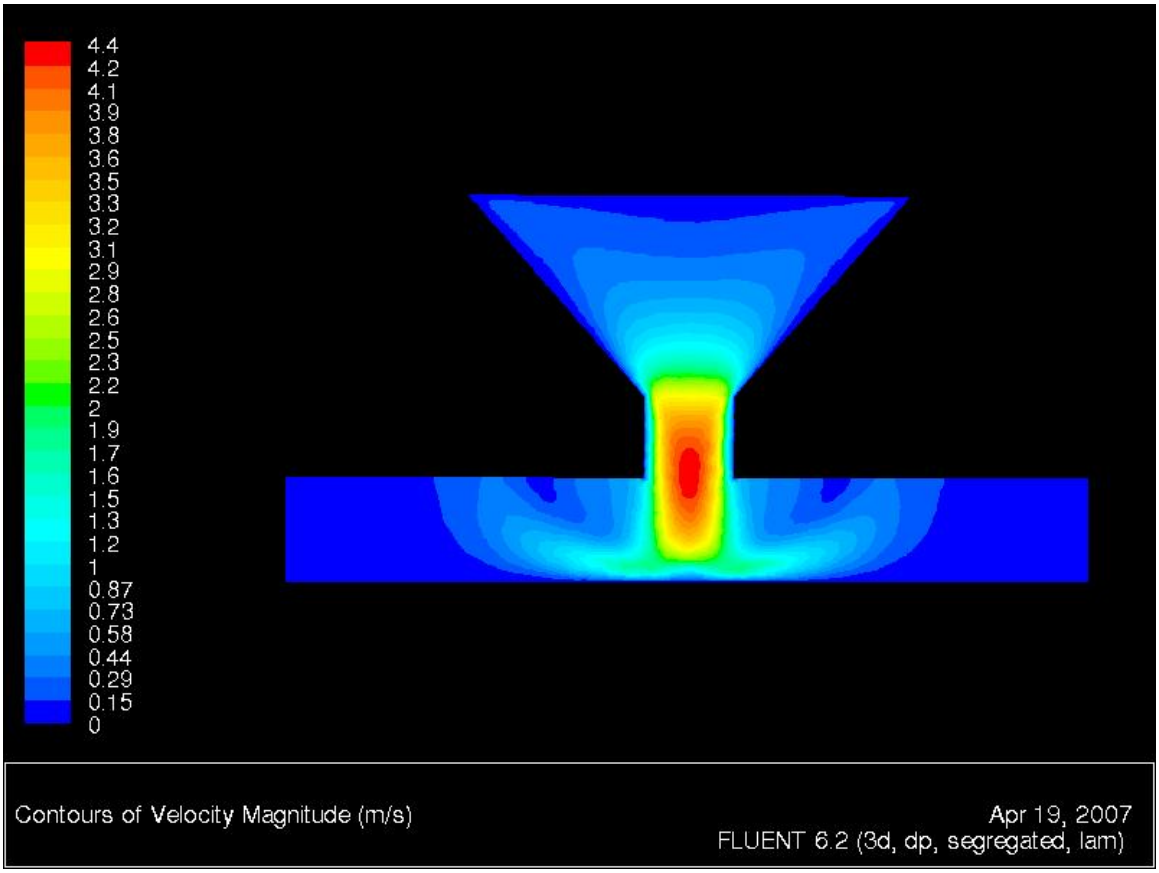

Figure 18. Fluent image showing 3D velocity profile at the impactor mid-plane

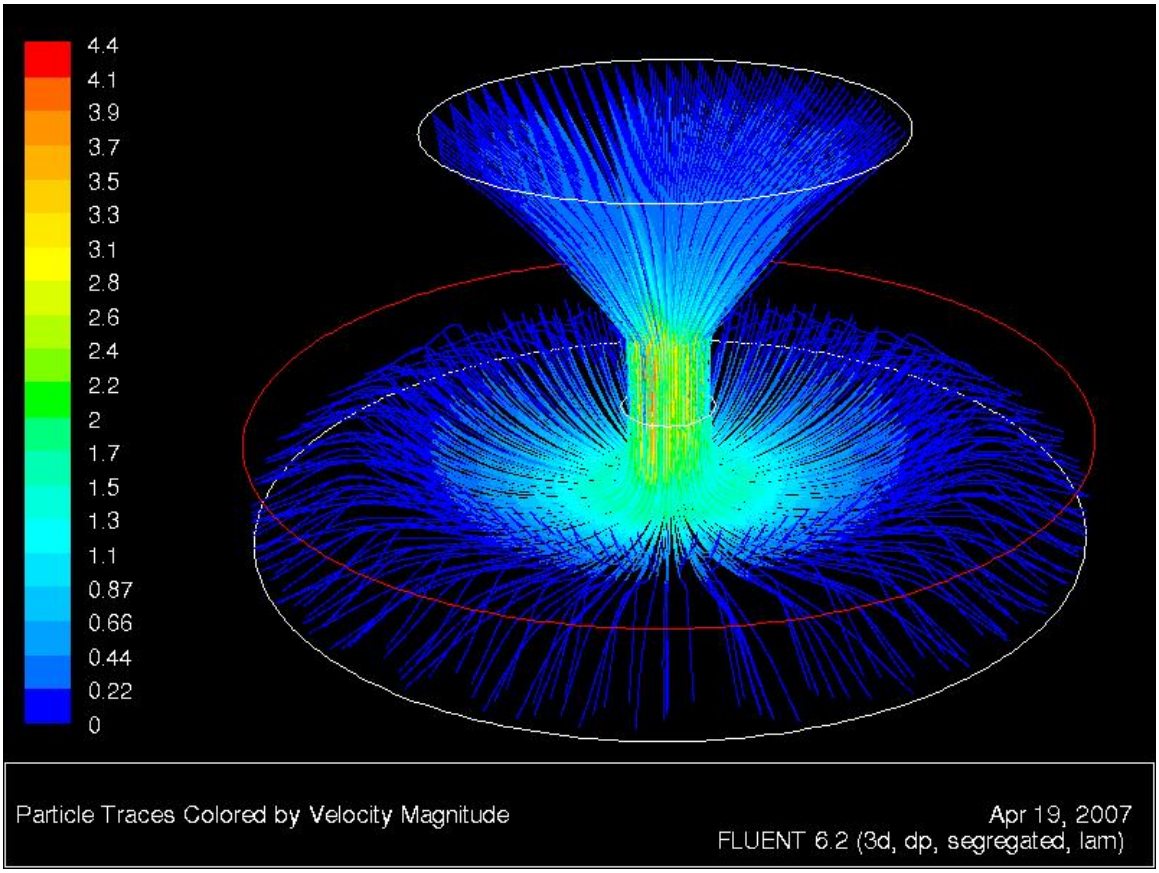

Figure 19. Fluent image showing smaller sized particle tracks (1 μm) through the impactor

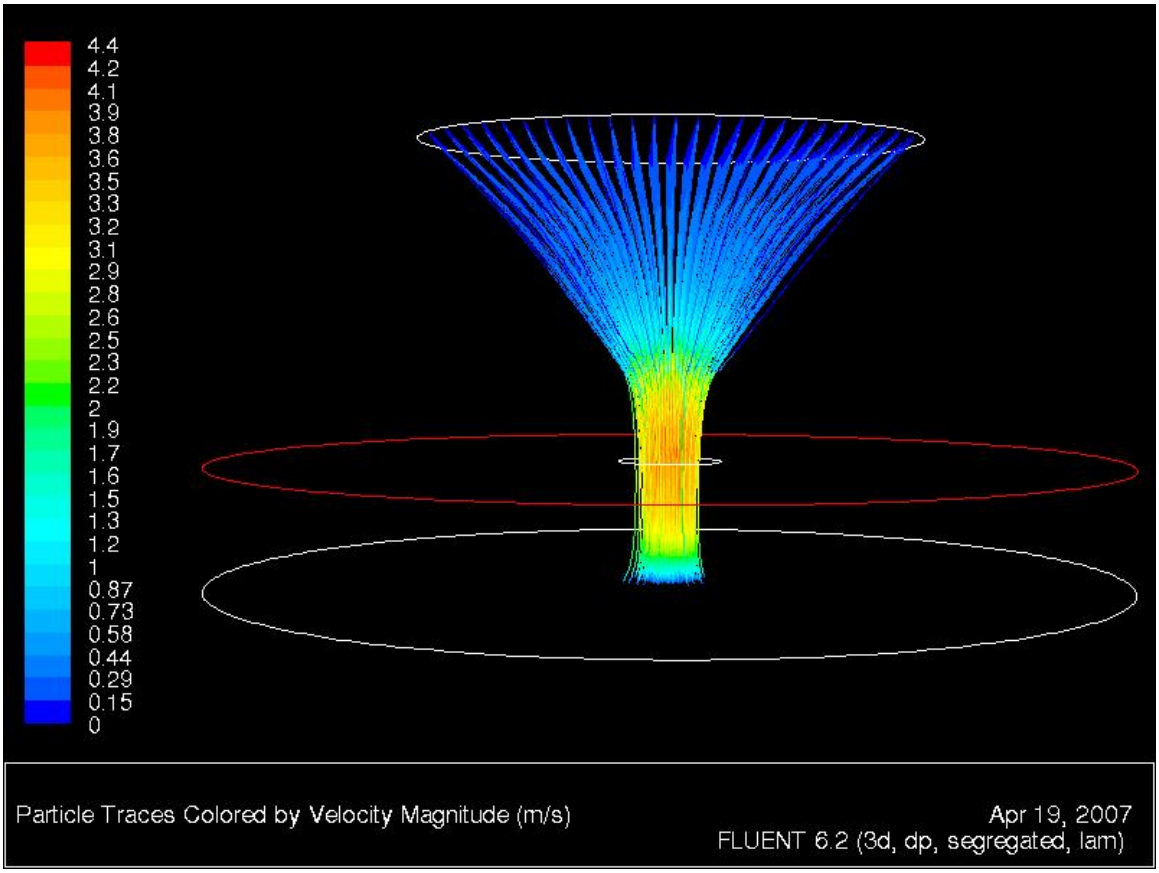

Figure 20. Fluent image showing larger sized (10 μm) particle tracks

VITA

Name	Mallika Mukundan
Address	Department of Mechanical Engineering, C/O Dr. Bing Guo Texas A&M University, 3123 TAMU College Station, TX-77843
Education	B.E, Maharaja Sayaji Rao University of Baroda, India-390008 2004 M.S, Texas A&M University College Station, TX 77843 2007